

## Article

# Anti-Melanogenic Effects of *Lilium lancifolium* Root Extract via Downregulation of PKA/CREB and MAPK/CREB Signaling Pathways in B16F10 Cells

Seokmuk Park <sup>1,†</sup>, Nayeon Han <sup>1,2,†</sup>, Jungmin Lee <sup>2</sup>, Jae-Nam Lee <sup>3</sup>, Sungkwan An <sup>4</sup> and Seunghee Bae <sup>1,\*</sup> 

<sup>1</sup> Department of Cosmetics Engineering, Konkuk University, 120 Neungdong-ro, Gwangjin-gu, Seoul 05029, Republic of Korea; ted968@konkuk.ac.kr (S.P.); nina1305@konkuk.ac.kr (N.H.)

<sup>2</sup> Dermato Bio, Inc., #505, Techno Cube, 13-18 Songdogwahak-ro 16beon-gil, Yeongsu-gu, Incheon 21984, Republic of Korea; jungmin-lee@skinbutak.com

<sup>3</sup> Department of Cosmetology, Graduate School of Engineering, Konkuk University, 120 Neungdong-ro, Gwangjin-gu, Seoul 05029, Republic of Korea; jn386@konkuk.ac.kr

<sup>4</sup> Eco Up Bio, Inc., 373 Chang-ui-ri, Seorak-myeon, Gapyeong-gun 477852, Republic of Korea; anxcompany@naver.com

\* Correspondence: sbae@konkuk.ac.kr

† These authors contributed equally to this work.

**Abstract:** Hyperpigmentation disorders causing emotional distress require the topical use of depigmenting agents of natural origin. In this study, the anti-melanogenic effects of the *Lilium lancifolium* root extract (LRE) were investigated in B16F10 cells. Consequently, a non-cytotoxic concentration of the extract reduced intracellular melanin content and tyrosinase activity in a dose-dependent manner, correlating with the diminished expression of core melanogenic enzymes within cells. LRE treatment also inhibited cyclic adenosine monophosphate (cAMP) response element-binding protein (CREB)/microphthalmia-associated transcription factor signaling, which regulates the expression of tyrosinase-related genes. Upon examining these findings from a molecular mechanism perspective, LRE treatment suppressed the phosphorylation of protein kinase A (PKA), p38, and extracellular signal-related kinase (ERK), which are upstream regulators of CREB. In addition, L-phenylalanine and regaloside A, specifically identified within the LRE using liquid chromatography-mass spectrometry, exhibited inhibitory effects on melanin production. Collectively, these results imply that LRE potentially suppresses cAMP-mediated melanogenesis by downregulating PKA/CREB and mitogen-activated protein kinase (MAPK)/CREB signaling pathways. Therefore, it can be employed as a novel therapeutic ingredient of natural origin to ameliorate hyperpigmentation disorders.

**Keywords:** melanogenesis; anti-melanogenic effect; melanin; B16F10;  $\alpha$ -melanocyte stimulating hormone ( $\alpha$ -MSH); *Lilium lancifolium*; L-phenylalanine; regaloside A



**Citation:** Park, S.; Han, N.; Lee, J.; Lee, J.-N.; An, S.; Bae, S. Anti-Melanogenic Effects of *Lilium lancifolium* Root Extract via Downregulation of PKA/CREB and MAPK/CREB Signaling Pathways in B16F10 Cells. *Plants* **2023**, *12*, 3666. <https://doi.org/10.3390/plants12213666>

Academic Editor: Ain Raal

Received: 19 September 2023

Revised: 18 October 2023

Accepted: 22 October 2023

Published: 24 October 2023



**Copyright:** © 2023 by the authors. Licensee MDPI, Basel, Switzerland. This article is an open access article distributed under the terms and conditions of the Creative Commons Attribution (CC BY) license (<https://creativecommons.org/licenses/by/4.0/>).

## 1. Introduction

Melanin is synthesized within specialized ovoid organelles called melanosomes, which are produced by dendritic melanocytes in the basal layer of the epidermis, constituting only 1% of the total composition [1]. Melanin produced within melanosomes is transported via dendrites to neighboring keratinocytes, where it accumulates in the perinuclear area of both keratinocytes and melanocytes and forms supranuclear “caps” recognized for their ability to shield DNA from ultraviolet (UV) rays [2]. In addition, melanin shields skin cells from the harmful effects of UV radiation, oxidative stress, and other environmental factors [3–5]. Eumelanin is a deep brown/black insoluble polymer, whereas pheomelanin is a light red/yellow soluble polymer containing sulfur [1,6–8]. Eumelanin plays a crucial role in protecting against and determining the color of the skin, hair, and eyes. Excessive melanin expression has been attributed to conditions, such as melanoma, freckles,

lentigo, and abnormal skin pigmentation [9–13]. Among these disorders, hyperpigmentation, which is characterized by the excessive production of melanin, frequently originates from increased melanocyte and tyrosinase activity [14,15]. Previous studies have explored hyperpigmentation-related diseases, such as melasma, post-inflammatory hyperpigmentation (PIH), and lentigines, each with distinct characteristics and potential side effects [16]. Melasma is a prevalent hyperpigmentation disorder that is frequently triggered by hormonal changes [15]. It can lead to emotional distress, diminished self-esteem, and feelings of frustration due to the noticeable visibility of the condition [17,18]. Addison's disease is a hormonal disorder that can cause increased melanin production. Side effects of Addison's disease include mental health disorders and abnormal menstrual cycles [15].

The  $\alpha$ -melanocyte-stimulating hormone ( $\alpha$ -MSH) is primarily used in cultured melanocytes as a cell model in vivo [19]. DNA damage and repair are associated with the stimulation of melanogenesis, supported by p53 activation, which leads to elevated levels of tyrosinase messenger RNA (mRNA) and protein [20]. Notably, p53 activation triggers transcription from the proopiomelanocortin (POMC) gene promoter, inducing the release of  $\alpha$ -MSH from keratinocytes, a pivotal inducer of melanogenesis [21].  $\alpha$ -MSH then stimulates the melanocortin-1 receptor (MC1R) in melanocytes, promoting eumelanin production [21]. Therefore, melanin reduction induced by  $\alpha$ -MSH can be a major strategy for pigment treatment.

Hydroquinone, kojic acid, ascorbic acid, and arbutin are hypopigmentation agents known for their potential to inhibit melanin production and are commonly used for skin whitening or depigmentation purposes [22,23]. However, these conventional pigment inhibitors have notable drawbacks, including skin irritation, high allergic reactivity, and adverse responses [24–27]. Hydroquinone is currently the benchmark standard topical drug for the treatment of hyperpigmentation disorders, such as melanosclerosis [28]. However, permanent depigmentation and exogenous ochronosis have been reported with prolonged use [29–32]. Its utilization is not legally available by prescription or OTC in the European Union, Australia, or Japan owing to its unknown safety profile [29,32,33]. Arbutin, a naturally occurring beta-D-glucopyranoside found in bearberry, cranberry, and blueberry leaves, is among the foremost effective over-the-counter (OTC) pigment-lightening ingredients, with a structure similar to that of hydroquinone [34–37]. It functions by decreasing tyrosinase activity without affecting messenger RNA expression or inhibiting melanosome maturation; however, caution is warranted as it may lead to paradoxical pigment darkening due to PIH [34,37]. Kojic acid, a hydrophilic fungal derivative obtained from *Aspergillus* and *Penicillium* species, is the second most effective OTC melanogenic agent [34,38]. It is attributed to the inhibition of tyrosinase activity upon binding to copper [39,40]. This interference with tyrosinase, a pivotal enzyme in melanin production, contributes to its anti-melanogenic effects [41]. Kojic acid is a widely recognized therapy for treating melasma [42]. However, specific issues have been raised as kojic acid is recognized as a sensitizer and has shown mutagenic properties in cell culture studies [43]. Considering the potential risks associated with these inhibitors, researchers have explored novel candidates that can effectively inhibit tyrosinase without causing adverse effects [44,45]. In this endeavor, plant biosynthesized metabolites have emerged as promising alternatives to synthetic analogs [46,47]. These natural compounds exhibit potential for the development of less hazardous and more effective solutions for skin lightening and hyperpigmentation treatment.

*Lilium lancifolium*, commonly known as the tiger lily, belongs to the Liliaceae family [48–50]. These plants are distributed and cultivated in various temperate regions, including Eastern Asia, Europe, and North America [48,51]. In China, *L. lancifolium* is known for its edible bulbs, which possess high nutritional and antioxidative properties [52]. Furthermore, traditional Korean medicine has recognized the potential of the *Lilium* species to treat inflammatory disorders [53]. The root of *L. lancifolium* Thunb has historically been used for various respiratory conditions [49,54]. Polysaccharides from *L. lancifolium* have various beneficial effects, such as diminishing nitric oxide production in macrophages [51,55,56]. The leaves, roots, and bulbs of *L. lancifolium* contain amino acids, polysaccharides, saponins,

phenylpropanoids, phenolics, and other constituents [57–60]. This composition suggests the potential capacity to improve skin conditions. However, the anti-melanogenic effects of *L. lancifolium* root extract (LRE) and the underlying molecular mechanisms have not yet been explored. Therefore, this study aimed to elucidate the potential of LRE as an agent for inhibiting hyperpigmentation and as a raw material for formulating whitening functional products in the pharmaceutical and cosmetic sectors.

## 2. Results

### 2.1. Effects of LRE on Cell Viability and Melanogenesis in B16F10 Cells

*Lilium* species contain numerous bioactive compounds, such as amino acids, polysaccharides, phenolics, and flavonoids [61]. Based on the abundance of these bioactive substances, cosmetic ingredients derived from *Lilium* plants have been utilized for anti-aging, radiation protection, moisturization, acne treatment, and hair growth promotion. However, no study has investigated the anti-melanogenic effects of *L. lancifolium* [62]. Prior to assessing the anti-melanogenic effects of LRE, its potential cytotoxicity was examined in B16F10 cells (Figure 1A). Cells were treated with various concentrations (0, 20, 50, 100, and 200  $\mu\text{g}/\text{mL}$ ) of LRE and  $\alpha$ -MSH (200 nM) for 48 h. No cytotoxic effect on B16F10 cells treated with doses below 100  $\mu\text{g}/\text{mL}$  of LRE was observed (Figure 1A). However, B16F10 cells treated with 200  $\mu\text{g}/\text{mL}$  of LRE exhibited a 17.25% reduction in cell viability compared to the untreated group. Moreover, co-treatment of LRE (200  $\mu\text{g}/\text{mL}$ ) and  $\alpha$ -MSH (200 nM) resulted in an 18.59% reduction in cell viability compared to the  $\alpha$ -MSH-treated group. Consequently, for subsequent experiments, LRE was utilized at concentrations below 100  $\mu\text{g}/\text{mL}$ .

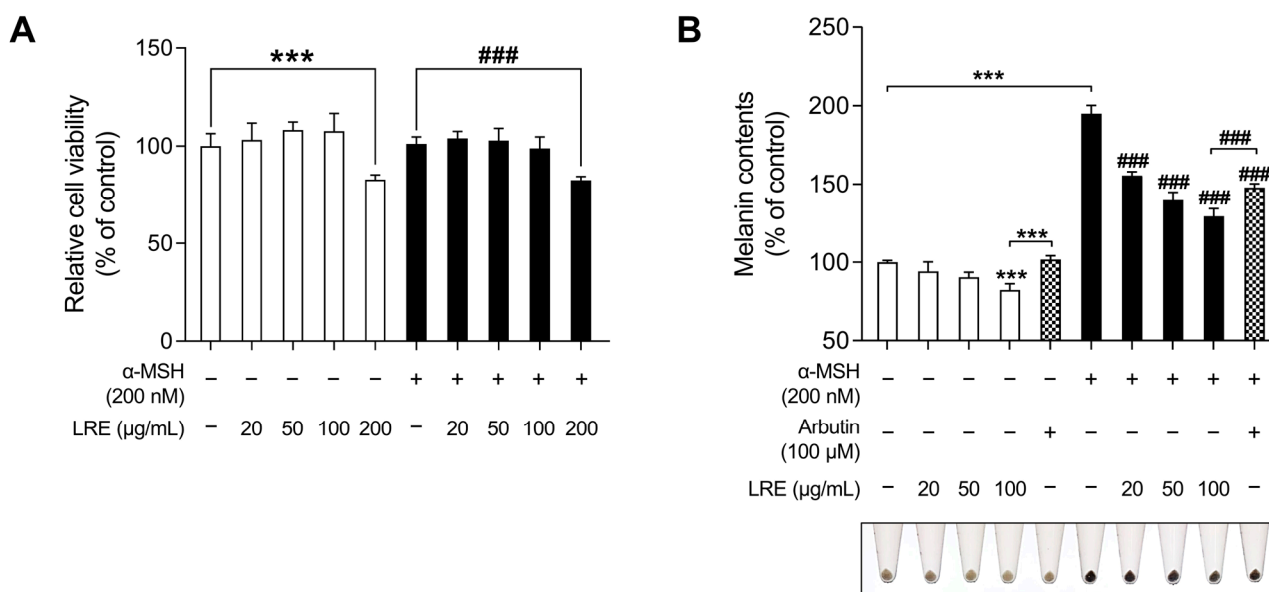


**Figure 1.** Effects of *Lilium lancifolium* (*L. lancifolium*) root extract on cell viability and melanin production in B16F10 cells. (A) B16F10 cells were seeded in 96-well plates ( $2 \times 10^3$  cells/well) and incubated for 24 h. The cells were treated with the indicated concentrations of LRE and  $\alpha$ -MSH for 48 h. Cell viability of B16F10 was measured via a WST-1 assay. (B) The cells were seeded in 60 mm dishes ( $1 \times 10^5$  cells) and incubated for 24 h. The cells were treated with indicated concentrations of LRE,  $\alpha$ -MSH, and arbutin for 48 h. Arbutin was utilized as the positive control. Intracellular melanin content was measured following stimulation with or without  $\alpha$ -MSH and subsequent treatment with LRE. The results are presented as the mean  $\pm$  SD of three independent experiments and were analyzed using a one-way analysis of variance followed by Tukey's test. LRE, *Lilium lancifolium* root extract; WST-1, water-soluble tetrazolium salt-1;  $\alpha$ -MSH, alpha-melanocyte-stimulating hormone. ###, \*\*\*  $p < 0.001$ .

Next, the effects of LRE on melanogenesis were evaluated. LRE significantly suppressed melanogenesis in B16F10 cells in a dose-dependent manner (Figure 1B). In the group treated with 100 µg/mL of LRE, there was a 17.76% reduction in the production of melanin compared to the untreated group. In a similar manner, co-treatment of LRE (100 µg/mL) and α-MSH (200 nM) demonstrated a 65.67% reduction in melanin content compared to the α-MSH-treated group. Arbutin (100 µM) was employed as the positive control group, and cells treated with LRE (100 µg/mL) exhibited a 19.43% reduction in melanin content compared to those treated with arbutin. Similarly, co-treatment of LRE (100 µg/mL) and α-MSH (200 nM) showed an 18.31% reduction in cellular melanin content compared to the group co-treated with α-MSH (200 nM) and arbutin (100 µM). These results suggest that the bioactive components of LRE may suppress melanin synthesis by inhibiting melanogenesis-related gene and protein expression.

### 2.2. Inhibitory Effects of LRE on the Expression of Melanogenic Enzymes

Tyrosinase, tyrosinase-related protein 1 (Tyrp1), and tyrosinase-related protein 2 (Tyrp2), collectively referred to as melanogenic enzymes, play crucial roles in pigmentation [63]. Tyrosinase catalyzes the conversion of tyrosine to 3,4-dihydroxyphenylalanine, which is a vital and rate-limiting step in melanin synthesis [64]. Similarly, Tyrp1 and Tyrp2, two other tyrosinase-related proteins, also contribute to eumelanin synthesis [65]. As LRE inhibited melanin production in B16F10 cells, we investigated whether LRE regulates the expression of melanogenic enzymes in these cells. LRE markedly suppressed cellular tyrosinase activity (Figure 2A). Cells treated with 100 µg/mL of LRE displayed a 36.33% reduction in cellular tyrosinase activity compared to the untreated group. Stimulation with α-MSH significantly increased tyrosinase enzyme function within the cells. Conversely, the co-treatment group with α-MSH (200 nM) and LRE (0–100 µg/mL) demonstrated a dose-dependent decrease in intracellular tyrosinase activity (Figure 2A). In the group co-treated with α-MSH and 100 µg/mL of LRE, an 81.91% reduction in tyrosinase activity was observed compared to the α-MSH-treated group. Similar to Figure 1B, LRE exerted a substantial inhibitory effect on cellular tyrosinase activity compared to the positive control, arbutin (100 µM). The LRE-induced reduction in tyrosinase activity can be attributed to a reduction in the expression and stability of melanogenic enzymes. To verify whether LRE reduced the expression of tyrosinase, Tyrp1, and Tyrp2 in B16F10 cells, Western blotting, reverse-transcription polymerase chain reaction (RT-PCR), and quantitative real-time polymerase chain reaction (qRT-PCR) assays were conducted following co-treatment with the specified concentrations of LRE and α-MSH. Our results revealed that LRE suppressed the mRNA expression of tyrosinase, Tyrp1, and Tyrp2 in B16F10 cells (Figures 2B and S1A). In particular, RT-PCR and qRT-PCR assays showed that the co-treatment group with α-MSH (200 nM) and LRE (50 and 100 µg/mL) exhibited a dose-dependent decrease in tyrosinase-related genes (Figures 2B and S1A). This effect was consistent with the inhibition of protein levels of tyrosinase, Tyrp1, and Tyrp2 (Figure 2C). Collectively, these findings suggest that the inhibition of melanogenesis by LRE can be attributed to the suppression of melanogenic enzyme activity and the downregulation of tyrosinase, Tyrp1, and Tyrp2 expression in B16F10 cells.

### 2.3. Inhibitory Effects of LRE on Cyclic Adenosine Monophosphate (cAMP) Response Element-Binding Protein (CREB)/Microphthalmia-Associated Transcription Factor (Mitf) Signaling Pathway

Recent studies have revealed the significance of Mitf expression in regulating melanogenic enzyme levels and influencing melanogenesis in B16F10 cells [66–68]. In addition, tyrosinase, Tyrp1, and Tyrp2 are the major targets of melanogenic enzymes induced by Mitf [69]. Under physiological conditions, the elevation in cAMP induced by α-MSH results in phosphorylation at the serine 133 residue of CREB via various signaling pathways [70–72]. This ultimately results in an increase in the transcriptional level of Mitf [73]. Therefore, we investigated whether LRE, which inhibits the expression of tyrosinase-related proteins, downregulated the CREB/Mitf signaling pathway. LRE decreased both Mitf mRNA and protein levels

(Figures 3A,B and S1B). In particular, the elevated protein and mRNA levels of Mitf induced by  $\alpha$ -MSH treatment were significantly reduced to levels comparable to those in the control group following LRE treatment. The phosphorylation level at the serine 133 residue of CREB, which is the most prominent transcription factor regulating the transcriptional level of Mitf, was assessed via Western blotting.  $\alpha$ -MSH (200 nM) treatment increased the phosphorylation levels of CREB compared to the untreated control cells; however, the cells co-treated with LRE significantly decreased the phosphorylation of CREB in a dose-dependent manner compared to the  $\alpha$ -MSH-treated cells (Figure 3C,D). Treatment with LRE (100  $\mu$ g/mL) also exhibited a time-dependent reduction in  $\alpha$ -MSH-induced Mitf and p-CREB protein expression (Figure 4A–C). These findings imply that LRE downregulates the expression of melanogenic enzymes via the CREB/Mitf signaling pathway.

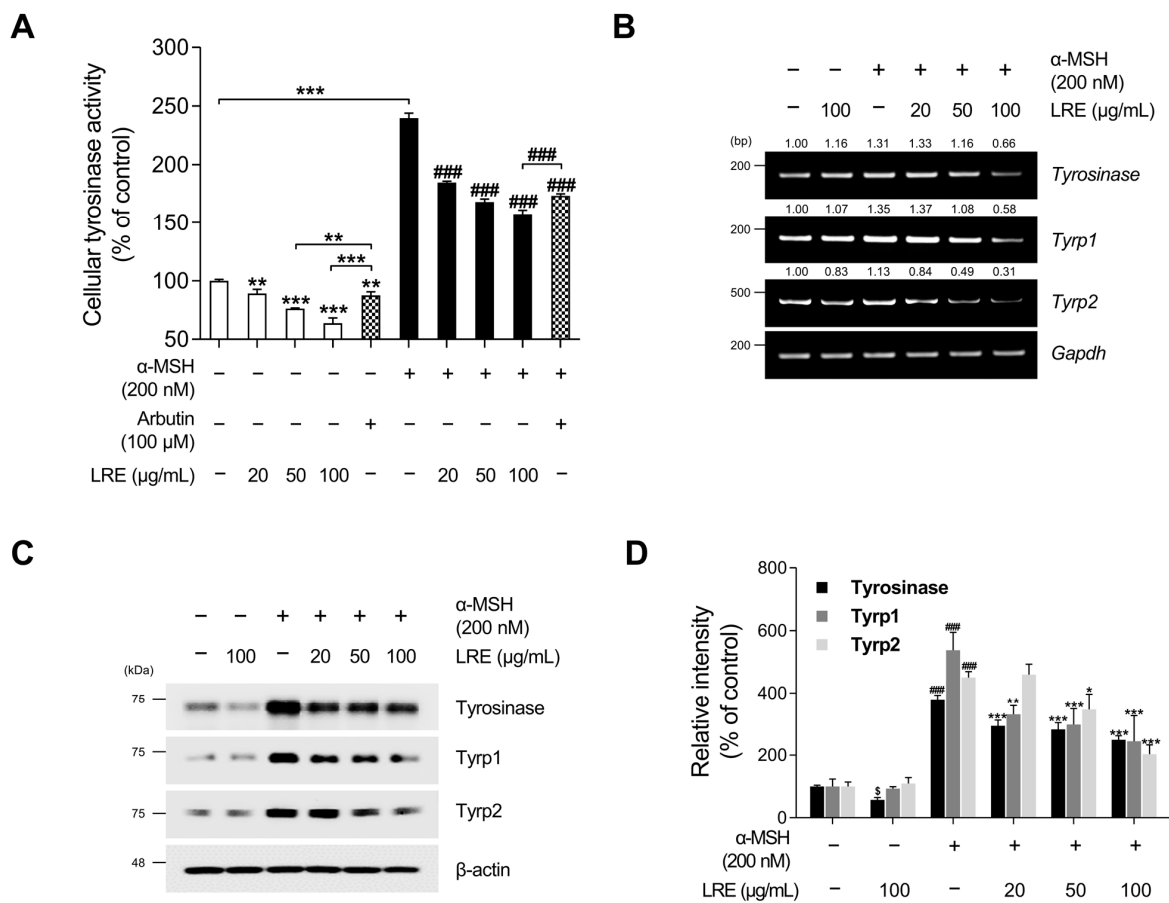


**Figure 2.** Effects of *L. lancifolium* root extract on cellular tyrosinase activity and melanogenic enzyme expression. (A) B16F10 cells were seeded in 60 mm dishes ( $1 \times 10^5$  cells) and incubated for 24 h. The cells were treated with the indicated concentrations of LRE,  $\alpha$ -MSH, and arbutin for 48 h. Intracellular tyrosinase activity was assessed following treatment of B16F10 cells with LRE and stimulation with or without  $\alpha$ -MSH. (B) B16F10 cells were seeded in 60 mm dishes ( $1 \times 10^5$  cells) and incubated for 24 h. The cells were then treated with the indicated concentrations of LRE and  $\alpha$ -MSH for 24 h. mRNA levels of tyrosinase-related genes (*tyrosinase*, *Tyrp1*, and *Tyrp2*) were detected via RT-PCR, with *GAPDH* serving as a loading control. (C) B16F10 cells were incubated with the indicated concentrations of LRE and  $\alpha$ -MSH for 48 h. Protein levels of tyrosinase-related enzymes (tyrosinase, Tyrp1, and Tyrp2) were analyzed via Western blotting, with  $\beta$ -actin serving as a loading control. (D) Quantitation of protein level was conducted using ImageJ software version 1.53t. The results are presented as the mean  $\pm$  SD of three independent experiments and were analyzed using a one-way analysis of variance followed by Tukey’s test. RT-PCR, reverse-transcription polymerase chain reaction; mRNA, messenger RNA. \$, \*  $p < 0.05$ ; \*\*  $p < 0.01$ ; ###, \*\*\*  $p < 0.001$ .



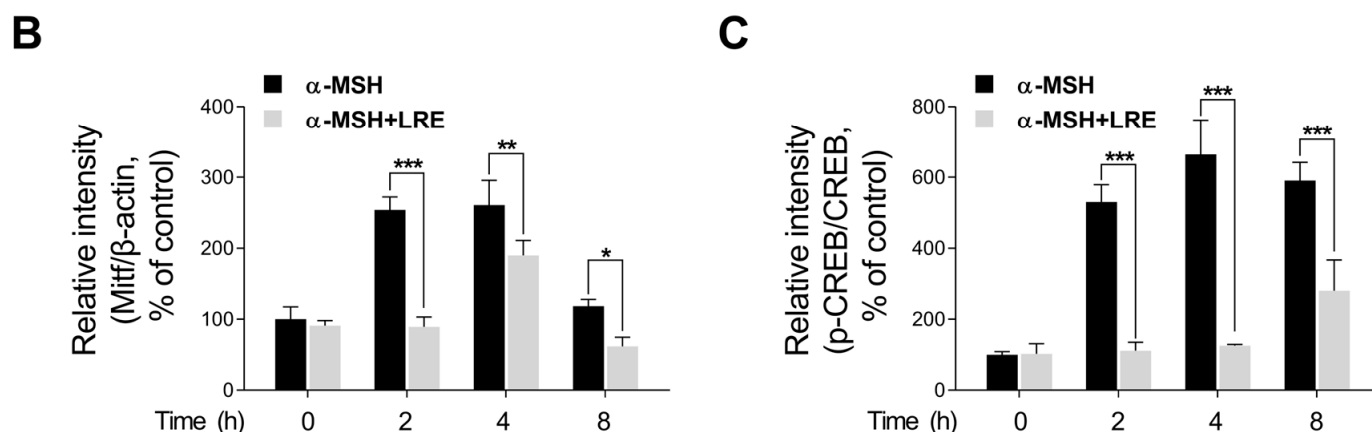


**Figure 4.** Effects of *L. lancifolium* root extract on the CREB/Mitf signaling pathway, depending on treatment duration. (A) Mitf, p-CREB, and CREB protein levels were examined at different time points after co-treatment with LRE (100 µg/mL) and α-MSH (200 nM). The protein levels were determined via Western blotting, while β-actin served as a loading control. (B,C) Quantitation of protein levels was conducted using ImageJ software version 1.53t. The results are presented as the mean ± SD of three independent experiments and were analyzed using a one-way analysis of variance followed by Tukey's test. \*  $p < 0.05$ ; \*\*  $p < 0.01$ ; \*\*\*  $p < 0.001$ .

#### 2.4. Inhibitory Effects of LRE on Protein Kinase A (PKA)/CREB and Mitogen-Activated Protein Kinase/CREB Signaling Pathways

Several kinases target CREB, a transcription factor that regulates the transcription of Mitf [73]. These regulators promote CREB phosphorylation at the serine 133 residue, activating CREB-dependent transcription [74]. Notably, the major kinases facilitating CREB phosphorylation and its subsequent binding to Mitf promoters are PKA, p38, and extracellular signal-related kinase (ERK) [74–76]. In particular, the α-MSH/MC1R pathway, the initial signaling pathway inducing melanogenesis in melanocytes, elevates intracellular cAMP levels [77]. Consequently, cAMP induces the phosphorylation of PKA, p38, and ERK, resulting in the transcriptional activation of CREB [78–81]. To comprehend the molecular mechanism by which LRE inhibits the phosphorylation of CREB at the serine 133 residue, the upstream kinases of CREB were assessed via Western blotting. LRE significantly reduced the phosphorylation of PKA, p38, and ERK in a dose-dependent manner (Figure 5A,B). In particular, the group treated with 100 µg/mL of LRE showed a significant decrease in the phosphorylation of PKA, p38, and ERK compared to the untreated control group. Treatment with α-MSH induced the phosphorylation of PKA at threonine 197, p38 at threonine 180 and tyrosine 180, and ERK at threonine 202 and tyrosine 204. However, cells co-treated with α-MSH and LRE displayed a considerable decrease in the phosphorylation levels of PKA, p38, and ERK (Figure 5A,B). Furthermore, whether the decreased phosphorylation of ERK, p38, and PKA was time-dependent was investigated. The phosphorylation levels of p38 and ERK were reduced in the α-MSH (200 nM) and LRE (100 µg/mL) co-treated group compared to those in the α-MSH-treated group at 2, 4, and 8 h (Figure 6A–D). In addition, the phosphorylation of PKA exhibited a similar decreasing trend at 4 h and 8 h. Collectively, these results suggest that LRE downregulates the CREB signaling pathway by inhibiting the PKA, p38, and ERK signaling pathways.

#### 2.5. Inhibitory Effects of LRE on cAMP-Mediated Melanogenesis in B16F10 Cells

cAMP acts as a secondary messenger and plays a significant role in regulating various functions in benign melanocytes and melanoma cells [82]. cAMP is generated from two distinct sources, transmembrane and soluble adenylyl cyclases, and its degradation is regulated by a family of proteins known as phosphodiesterases [83]. Recent studies have indicated that distinct cAMP signaling pathways promote pigmentation by modifying the expression of melanogenic genes [84]. While the α-MSH/MC1R signaling pathway mediates

the crucial regulatory mechanism of melanin production, several cAMP-inducing agents, such as dibutyryl-cAMP (dbcAMP), forskolin, and 3-isobutyl-1-methylxanthine (IBMX), are widely employed in both in vitro and in vivo melanogenic-mimic models [85–87]. Thus, we investigated whether LRE, which inhibits  $\alpha$ -MSH-induced melanogenesis, exerts an anti-melanogenic effect on other cAMP-mediated melanogenesis pathways. The groups treated with cAMP-inducing agents (dbcAMP, IBMX, and FSK) exhibited a substantial increase in cellular melanin content (Figure 7A); however, the groups co-treated with cAMP inducers and LRE showed a reduction in melanin content compared to the negative control groups. In addition, cAMP inducers increased cellular tyrosinase activity; however, these effects were markedly decreased in cells co-treated with cAMP inducer and LRE in a dose-dependent manner (Figure 7B). These findings suggest the potential of LRE as a natural anti-melanogenic agent that can inhibit cAMP-mediated melanogenesis.

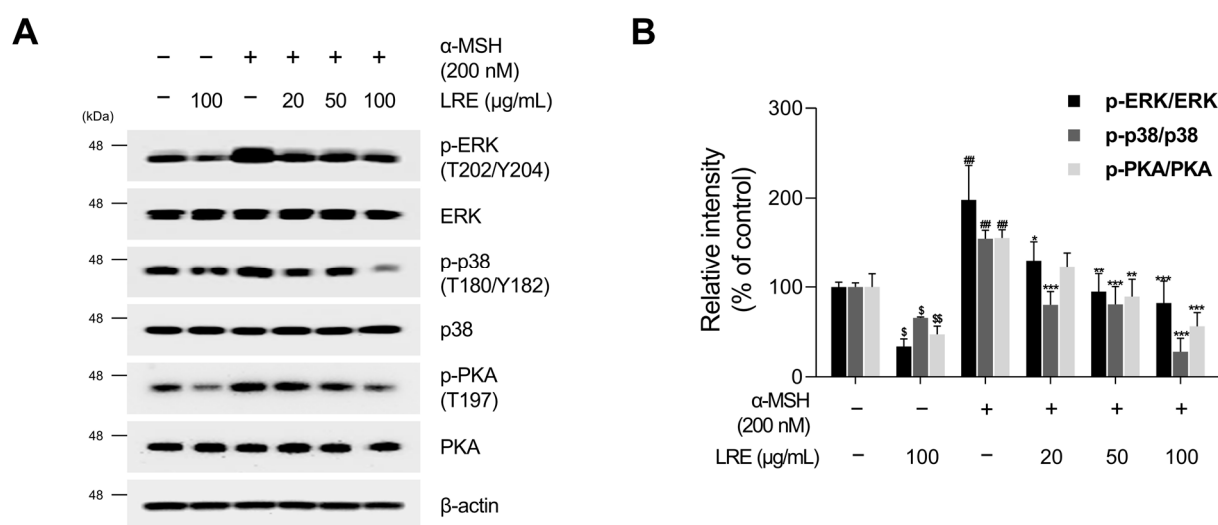
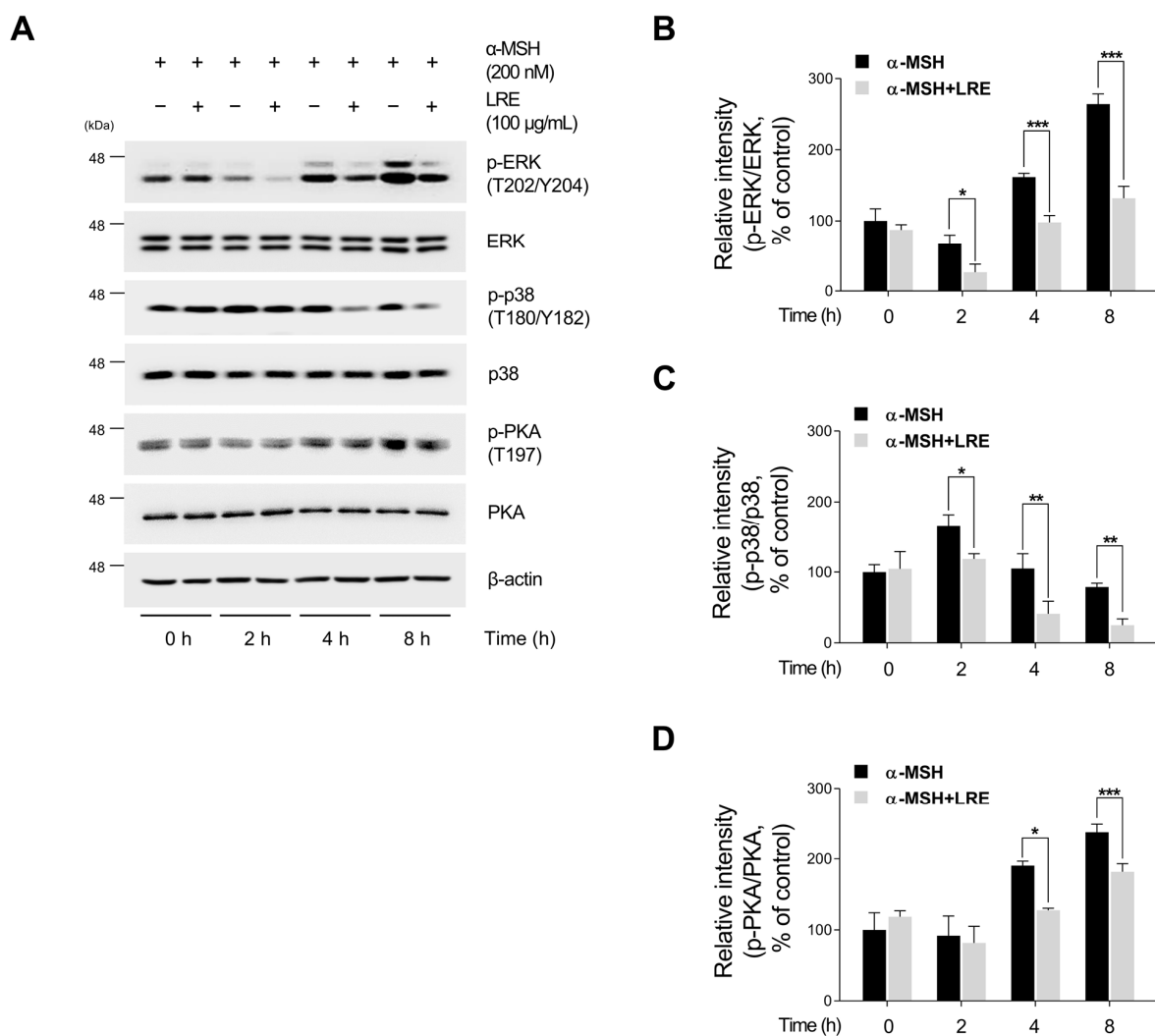


**Figure 5.** Effects of *L. lancifolium* root extract on the PKA/CREB and MAPK/CREB signaling pathways. (A) B16F10 cells were seeded in 60 mm dishes ( $2 \times 10^5$  cells) and incubated for 24 h. The cells were treated with the indicated concentrations of LRE and  $\alpha$ -MSH for 12 h. The protein levels of CREB upstream signaling were assessed via Western blotting, with  $\beta$ -actin serving as a loading control. (B) Protein levels were quantified using ImageJ software version 1.53t. The results are presented as the mean  $\pm$  SD of three independent experiments and were analyzed using a one-way analysis of variance followed by Tukey's test. PKA, protein kinase A; MAPK, mitogen-activated protein kinase. \*, \$  $p < 0.05$ ; \*\*, ##, \$\$  $p < 0.01$ ; \*\*\*  $p < 0.001$ .

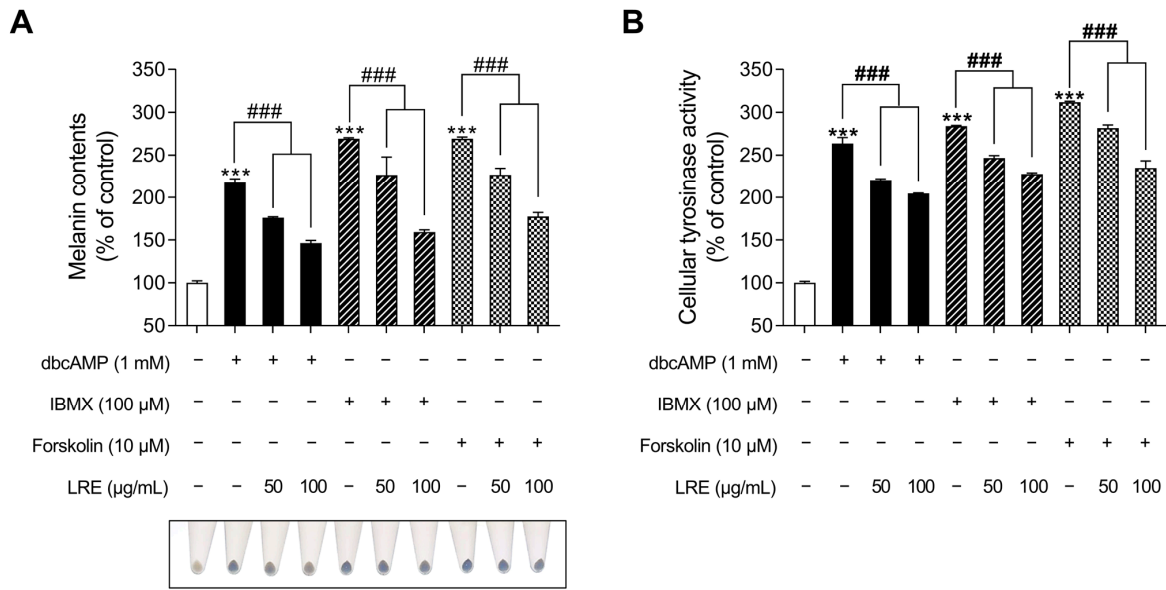
## 2.6. Characterization of LRE via High-Performance Liquid Chromatography-High-Resolution Mass Spectrometry Analysis

Table 1 and Figure 8 present the various organic compounds identified in the LRE using high-performance liquid chromatography-high-resolution mass spectrometry (HPLC-HRMS). The HRMS conditions and chromatographic separation were carried out using an ACQUITY BEH C18 column (1.7  $\mu$ m, 150  $\times$  2.1 mm) with a 2  $\mu$ L injection of LRE. Mass spectrometry acquisition was performed in the positive ion mode, covering the  $m/z$  range of 150 to 1500. Data analysis for all LRE compositions was conducted using Xcalibur software version 4.3. Figure 8 demonstrates the presence of 13 main compositions in the LRE, and retention times (RTs) for analytes are reported in Table 1. Out of these, two are unknown compounds with RTs of 8.03 and 12.78, and their molecular compositions are  $C_{69}H_{75}O_7$  and  $C_{83}H_{85}O_3$ , respectively. The analytes of interest included various amino acid analogs, namely L-alanyl-L-alpha-aspartyl-L-proline, methyl N-acetylhistidinate, L-phenylalanine, Boc-O-methyl-L-threonine, threonyl- $\alpha$ -glutamylleucine, Boc-Lys(Z)-OH, Z-L-Pro-L-Leu-Gly, Methyl (4S)-4-[(2-pyridinylcarbonyl)amino]-L-prolinate, and L-Lysyl-L-leucyl-L-valyl-L-leucyl-L-alanyl-L-serine, all of which were found within the LRE. Notably,

regaloside A, a distinctive bioactive component previously reported in another study, was detected in the LRE [88]. These findings indicate that the organic compounds in the LRE possess anti-melanogenic effects in B16F10 cells. Based on these data, we analyzed the effects of L-phenylalanine and regaloside A on cell viability and its anti-melanogenic properties in B16F10 cells. A WST-1-based cytotoxicity assay revealed the non-toxic nature of L-phenylalanine and regaloside A, with concentrations of up to 500  $\mu\text{M}$  and 200  $\mu\text{M}$ , respectively (Figure 9A,C). Subsequently, whether L-phenylalanine and regaloside A downregulate melanin synthesis was investigated. L-phenylalanine and Regaloside A significantly attenuated melanin content compared with the  $\alpha$ -MSH-induced negative control group (Figure 9B,D). Our results are consistent with a previous study that suggests L-phenylalanine decreases melanin synthesis by inhibiting the uptake of tyrosine [89]. Taken together, these results suggest that LRE, which contains diverse organic compounds, such as glucosides and amino acids, along with regaloside A, may exhibit synergistic anti-melanogenic effects in B16F10 cells.



**Figure 6.** Effects of *L. lancifolium* root extract on the PKA/CREB and MAPK/CREB signaling pathways depending on treatment duration. (A) B16F10 cells were seeded in 60 mm dishes ( $2 \times 10^5$  cells) and incubated for 24 h. The cells were treated with the indicated concentrations of LRE and  $\alpha$ -MSH for 2, 4, and 8 h. The protein levels of CREB upstream signaling were assessed via Western blotting, with  $\beta$ -actin serving as a loading control. (B–D) Protein levels were quantified using ImageJ software version 1.53t. The results are presented as the mean  $\pm$  SD of three independent experiments and were analyzed using a one-way analysis of variance followed by Tukey's test. ERK, extracellular signal-related kinase. \*  $p < 0.05$ ; \*\*  $p < 0.01$ ; \*\*\*  $p < 0.001$ .



**Figure 7.** Effects of *L. lancifolium* root extract on cAMP-mediated melanogenesis. (A) B16F10 cells were seeded in 60 mm dishes ( $1 \times 10^5$  cells) and incubated for 24 h. The cells were treated with indicated concentrations of LRE and cAMP inducer (dbcAMP, IBMX, and FSK) for 48 h. Intracellular melanin contents were determined following stimulation with or without cAMP inducer and treatment with LRE. (B) The cells were seeded in 60 mm dishes ( $1 \times 10^5$  cells) and incubated for 24 h. The cells were treated with the indicated concentrations of LRE and cAMP inducer for 48 h. Intracellular tyrosinase activity was determined following treatment of B16F10 cells with LRE and stimulation with or without cAMP inducer. The results are presented as the mean  $\pm$  SD of three independent experiments and were analyzed using a one-way analysis of variance followed by Tukey’s test. dbcAMP, dibutyryl-cAMP; IBMX, 3-isobutyl-1-methylxanthine; FSK, forskolin; cAMP, cyclic adenosine monophosphate. \*\*\*, ###  $p < 0.001$ .

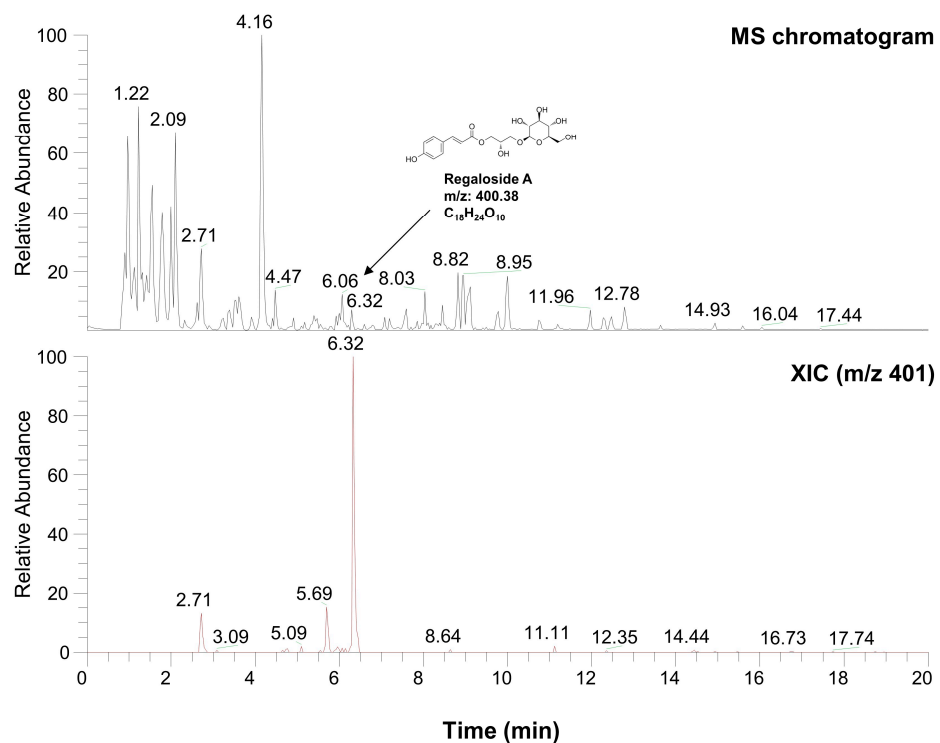


**Figure 8.** Characterization of compounds from *L. lancifolium* extract using high-performance liquid chromatography-high-resolution mass spectrometry analysis.

**Table 1.** High-resolution mass spectrometry data of identified molecules in *L. lancifolium* extract.

Number	Name	Formula	M.W.	RT (min)
1	L-alanyl-L-alpha-aspartyl-L-proline	C <sub>12</sub> H <sub>19</sub> O <sub>6</sub> N <sub>3</sub>	301.296	1.22
2	Methyl N-acetylhistidinate	C <sub>9</sub> H <sub>13</sub> O <sub>3</sub> N <sub>3</sub>	211.218	1.68
3	L-phenylalanine	C <sub>9</sub> H <sub>11</sub> NO <sub>2</sub>	165.189	2.09
4	Threonyl- $\alpha$ -glutamylleucine	C <sub>15</sub> H <sub>27</sub> O <sub>7</sub> N <sub>3</sub>	361.391	2.71
5	Boc-O-methyl-L-threonine	C <sub>10</sub> H <sub>19</sub> NO <sub>5</sub>	234.133	4.16
6	Hopantenic acid glucoside	C <sub>16</sub> H <sub>29</sub> O <sub>10</sub> N	395.402	4.47
7	Methyl (4S)-4-[(2-pyridinylcarbonyl)amino]-L-prolinate	C <sub>12</sub> H <sub>15</sub> O <sub>3</sub> N <sub>3</sub>	250.118	6.06
8	Regaloside A	C <sub>18</sub> H <sub>24</sub> O <sub>10</sub>	400.377	6.32
9	Boc-Lys(Z)-OH	C <sub>19</sub> H <sub>28</sub> O <sub>6</sub> N <sub>2</sub>	380.435	8.82
10	Z-L-Pro-L-Leu-Gly	C <sub>21</sub> H <sub>29</sub> O <sub>6</sub> N <sub>3</sub>	419.471	8.95
11	L-Lysyl-L-leucyl-L-valyl-L-leucyl-L-alanyl-L-serine	C <sub>29</sub> H <sub>55</sub> O <sub>8</sub> N <sub>7</sub>	629.789	11.96

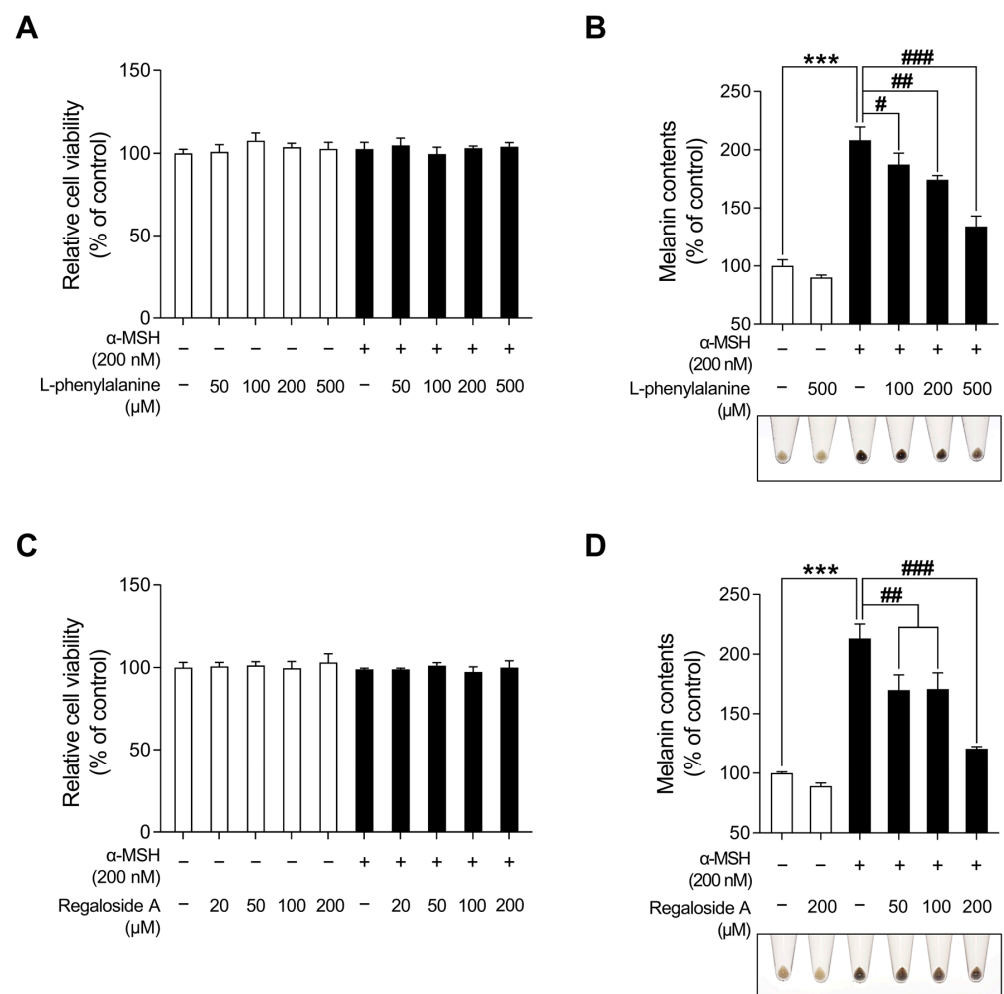


**Figure 9.** Effects of L-phenylalanine and regaloside A on cell viability and melanin production in B16F10 cells. (A,C) B16F10 cells were seeded in 96-well plates ( $2 \times 10^3$  cells/well) and incubated for 24 h. The cells were treated with the indicated concentrations of L-phenylalanine or regaloside A, with or without  $\alpha$ -MSH for 48 h. Cell viability of B16F10 was measured via the WST-1 assay. (B,D) The cells were seeded in 60 mm dishes ( $1 \times 10^5$  cells) and incubated for 24 h. The cells were treated with the indicated concentrations of L-phenylalanine or regaloside A, with or without  $\alpha$ -MSH for 48 h. Intracellular melanin contents were determined following stimulation with or without  $\alpha$ -MSH and treatment with L-phenylalanine or regaloside A. The results are presented as the mean  $\pm$  SD of three independent experiments and were analyzed using a one-way analysis of variance analysis followed by Tukey's test. #  $p < 0.05$ ; ##  $p < 0.01$ ; \*\*\*, ###  $p < 0.001$ .

### 3. Discussion

Despite numerous studies elucidating the beneficial physiological effects of *L. lancifolium*, including its anti-inflammatory and antioxidant properties, there is a scarcity of research on its physiological interactions within the skin [56,58,90]. Notably, the leaves, roots, and bulbs of *L. lancifolium* have been utilized in medicinal practices in Northeast Asia and are recognized for their amino acids, polysaccharides, saponins, phenylpropanoids, phenolics, and other compounds, suggesting their potential to ameliorate skin conditions [57–60]. Therefore, this study aimed to investigate the anti-melanogenic effects of *L. lancifolium* on B16F10 cells, anticipating its physiological role in the skin. Water was used as the extraction solvent for this purpose.

Skin pigmentation is a highly conserved defense mechanism in skin tissues against deleterious factors, such as UV radiation [91]. However, excessive melanin production can result in pigmentary disorders, such as hyperpigmentation, melasma, and solar lentigines [92,93]. Considering the impact of facial hyperpigmentation on the quality of life of patients, there is an imperative need for novel cosmetic ingredients derived from natural sources to alleviate hyper-melanogenic conditions [94]. Therefore, we investigated the anti-melanogenic effects of LRE in B16F10 cells. Our findings demonstrated that LRE effectively reduced melanin production in a dose-dependent manner without causing cytotoxicity (Figure 1A,B). In previous studies, representative melanogenic enzymes, including tyrosinase, Tyrp1, and Tyrp2, have been identified as crucial elements that upregulate melanogenesis in melanocytes. Therefore, we examined whether the LRE-induced reduction in melanin production could be attributed to the downregulation of these melanogenic enzymes. Our results revealed that LRE reduced cellular tyrosinase activity as well as the mRNA and protein levels of tyrosinase, Tyrp1, and Tyrp2 in a dose-dependent manner (Figure 2A–D). Furthermore, the melanin-reducing efficacy of LRE (100 µg/mL) notably surpassed that of arbutin (100 µM). This emphasizes the potential of LRE to efficiently exert anti-melanogenic effects by impeding the expression of core melanogenic enzymes in B16F10 cells.

The intricate process of melanogenesis is governed by an enzymatic cascade, including tyrosinase, which is modulated by transcription factors, such as Mitf and CREB [72].  $\alpha$ -MSH binding to MC1R triggers cAMP production, which induces the phosphorylation of the CREB transcription factor, increasing Mitf expression. Mitf binds to the promoter regions of melanin-producing genes and positively regulates the transcription of tyrosinase, Tyrp1, and Tyrp2 [67,72,95,96]. Therefore, inhibition of cAMP/CREB/Mitf signaling in B16F10 cells has been explored in various studies as a therapeutic strategy for mitigating hyperpigmentation [97,98]. In this study, LRE effectively attenuated CREB/Mitf in a time- and dose-dependent manner both in the presence and absence of  $\alpha$ -MSH treatment (Figures 3 and 4C). In particular, co-treatment with LRE and  $\alpha$ -MSH exhibited a reduction in the phosphorylation level of CREB at the serine 133 residue, which was elevated by  $\alpha$ -MSH treatment. In addition, Mitf protein stability was reduced by LRE treatment (Figure 3B). These findings suggest that LRE inhibits melanogenesis by effectively attenuating the CREB/Mitf signaling pathway.

Multiple kinases have been identified as regulators of CREB, the transcription factor modulating the transcriptional level of Mitf [73]. Several studies have demonstrated that the key kinases, such as PKA, p38, and ERK, are phosphorylated by increased cAMP levels induced by  $\alpha$ -MSH, ultimately enhancing the CREB/Mitf pathway [74–76,78–80]. Therefore, to comprehend the molecular mechanism by which LRE inhibits the phosphorylation of CREB at the serine 133 residue, the upstream kinases of CREB were assessed using Western blotting. Our findings demonstrated that LRE reduced the phosphorylation levels of ERK, p38, and PKA, even when administered as a single treatment. Furthermore, LRE decreased the elevated phosphorylation levels of ERK, p38, and PKA induced by  $\alpha$ -MSH treatment (Figure 5A,B). In addition, co-treatment with LRE decreased the phosphorylation levels of ERK, p38, and PKA, which were elevated by  $\alpha$ -MSH (200 nM) treatment at 4 h and 8 h (Figure 6A–D). Collectively, these findings suggest that LRE inhibits Mitf

expression and melanin synthesis by suppressing the PKA/CREB and mitogen-activated protein kinase (MAPK)/CREB signaling pathways. Subsequently, to confirm whether the anti-melanogenic effect of LRE occurs in melanogenesis models stimulated by cAMP-inducing agents distinct from  $\alpha$ -MSH, melanin content and cellular tyrosinase assays were performed. LRE inhibited melanogenesis induced by dbcAMP, IBMX, and forskolin in a dose-dependent manner (Figure 7A,B). These results suggest that LRE inhibits cAMP-mediated melanogenesis through the PKA/CREB and MAPK/CREB signaling pathways. Further in-depth validation of the role of LRE in PKA, ERK, and p38 phosphorylation is required.

Furthermore, HPLC-HRMS analysis revealed the presence of various amino acid analogs, including L-phenylalanine, within the LRE. Regaloside A, a bioactive compound unique to *L. lancifolium*, was also present in the LRE [56,88,99]. L-phenylalanine and regaloside A from LRE exhibited potential anti-melanogenic properties in the melanin content assay; however, additional validation is necessary to assess its reliability regarding its anti-melanogenic effects on B16F10 cells and how it affects skin whitening [89].

In this study, we found that LRE may alleviate hyperpigmentation by decreasing the levels of core melanogenic elements in cultured B16F10 cells. Despite a single treatment, LRE decreased CREB/Mitf signaling, along with the phosphorylation levels of its upstream signaling proteins, such as PKA, ERK, and p38. Consequently, LRE exhibited a stronger anti-melanogenic effect than arbutin regarding melanin synthesis and intracellular tyrosinase activity. The therapeutic effects of LRE on skin whitening and its definitive molecular mechanisms require further evaluation.

In conclusion, this study provided the first evidence that LRE has the potential to be an effective and safe depigmenting agent. We also demonstrated the anti-melanogenic effects of LRE as a novel cosmetic ingredient that overcomes the side effects of conventional whitening treatments.

## 4. Materials and Methods

### 4.1. Cell Culture and Preparation of *L. lancifolium* Extract

B16F10 murine melanoma cells were procured from ATCC (Manassas, VA, USA). The cells were cultured in Dulbecco's Modified Eagle's medium (Gibco, Grand Island, NY, USA) supplemented with 10% fetal bovine serum (Gibco), 1% streptomycin (100 mg/mL) (Gibco), and penicillin (100 U/mL) (Gibco) at 37 °C in a humid environment with 5% CO<sub>2</sub>. The root of *Lilium lancifolium* utilized in this study was obtained from a cultivation site located in the Pyeongchang region (Gangwon-do, Republic of Korea) in May 2022. The extraction method of *L. lancifolium* root was performed according to the previously described method [100]. After three cycles of rinsing with distilled water, the plants were left to air dry at room temperature. Ten grams of dried *L. lancifolium* root were chopped and subsequently finely pulverized into a fine powder using a grinder (SMX-3500GN, Shinil Industrial Co. Ltd., Seoul, Republic of Korea). Following this, the finely ground *L. lancifolium* root powder (10 g) was mixed with 200 mL of hot distilled water (80 °C) and left to steep for 4 h. The mixture was initially filtered using Whatman filter paper No. 1 (Whatman, Maidstone, UK) and subsequently, an additional purification step was carried out by subjecting it to ultrafiltration through a sterile 0.2  $\mu$ m bottle-top vacuum filter (Corning, Corning, NY, USA). Then, the filtrate was concentrated using a Rotavapor R-100 rotary evaporator (Buchi, Flawil, Switzerland) under vacuum and then lyophilized in a TFD-100 Freeze Dryer (ilShinBioBase Co., Ltd., Yangju-si, Republic of Korea) for 48 h. The lyophilized water extract from *L. lancifolium* root can be obtained at 1.58 g and the 1 g of freeze-dried water extract was diluted with 10 mL PBS at a concentration of 100 mg/mL. The extracted *L. lancifolium* root was aliquoted into 1 mL portions and stored at -20 °C until use.

#### 4.2. HPLC-HRMS Analysis

HPLC-HRMS analysis was conducted following a previously described method [100]. The chemical profiles of LRE were examined using a Thermo Ultimate-3000 UPLC system (Thermo Fisher Scientific, Waltham, MA, USA) coupled with Thermo LTQ-Orbitrap XL (Thermo Fisher Scientific) and executed utilizing an ACQUITY BEH C18 column (1.7  $\mu\text{m}$ , 150 mm  $\times$  2.1 mm). The gradient conditions were established in the following sequence: 0 min (5% B), 0–5 min (5% B), 5–20 min (70% B), and 20–27 min (100% B). The flow rate was set to 0.4 mL/min, with an injection volume of 2  $\mu\text{L}$ . The scan range was  $m/z$  150–1500 and MS experiments were performed in positive ion mode under the following conditions: FWHM resolution, 60,000; spray voltage, 4.0 kV; capillary voltage 35 V; and capillary temperature 300  $^{\circ}\text{C}$ . The data analysis was carried out utilizing the Xcalibur software (Version 4.3, Thermo Finnigan, San Jose, CA, USA). Regaloside A (MedChemExpress, Monmouth Junction, NJ, USA), known to be uniquely present in *L. lancifolium*, was utilized for quality assessment of its extract through HPLC-HRMS analysis [56].

#### 4.3. Cell Viability Assay

To analyze the effect of LRE on cell viability, B16F10 cells treated with LRE were assessed using the WST-1 assay. Briefly, B16F10 cells ( $3 \times 10^3$  cells/well) were initially seeded within a 96-well plate and maintained at 37  $^{\circ}\text{C}$  for 24 h. Subsequently, they were treated with various concentrations of LRE (0–1000  $\mu\text{g}/\text{mL}$ ) and maintained for 24 h and 48 h. After incubation, a solution of EZ-Cytox (100  $\mu\text{L}/\text{well}$ ) (DoGenBio, Seoul, Republic of Korea) was added to each well and the mixture was incubated for 30 min at 37  $^{\circ}\text{C}$ . Cell viability was detected by measuring absorbance at 450 nm using a Synergy<sup>TM</sup> HTX Multi-Mode Microplate Reader (Bioteck, Winooski, VT, USA).

#### 4.4. Measurement of Intracellular Melanin Content

Measurement of melanin content was conducted following a previously described method with a slight modification [101]. B16F10 cells ( $0.5 \times 10^5$  cells/mL) were seeded in a 60 mm plate and incubated at 37  $^{\circ}\text{C}$  for 24 h. Afterward, the cells were treated with or without 200 nM  $\alpha$ -MSH (Sigma-Aldrich, St. Louis, MO, USA), and then subjected to treatment with various concentrations of LRE (0–1000  $\mu\text{g}/\text{mL}$ ), regaloside A (0–200  $\mu\text{M}$ ), or L-phenylalanine (0–500  $\mu\text{M}$ ) (DaejungChemicals, Siheung-si, Republic of Korea). Arbutin (Sigma-Aldrich) was employed as a positive control, while  $\alpha$ -MSH (Sigma-Aldrich), dbcAMP (MedChemExpress), IBMX (Sigma-Aldrich), and forskolin (Sigma-Aldrich) were used as negative controls. After 48 h of incubation, the medium was carefully removed, and the cells were washed twice with PBS. Cell pellets were photographed and dissolved in 1 N NaOH lysis buffer at 100  $^{\circ}\text{C}$  for 30 min. The dissolved melanin content was measured at 450 nm using a microplate reader.

#### 4.5. Measurement of Tyrosinase Activity Assay

Intracellular tyrosinase activity was measured following a previously described method with a slight modification [41]. B16F10 cells ( $0.5 \times 10^5$  cells/mL) were seeded in a 60 mm plate and cultured for 24 h. Subsequently, the cells were stimulated with or without 200 nM  $\alpha$ -MSH, and then treated with various concentrations of LRE (0–1000  $\mu\text{g}/\text{mL}$ ), regaloside A (0–200  $\mu\text{M}$ ), or L-phenylalanine (0–500  $\mu\text{M}$ ). After 48 h, the cells were washed twice with PBS and then lysed with RIPA buffer (containing 50 mM pH 7.4 Tris hydrochloride, 150 mM sodium chloride, 1% NP-40, 0.5% sodium deoxy cholate, 0.1% sodium dodecyl sulfate) for 1 h. The lysates were then centrifuged at  $10,000 \times g$  for 30 min. The dissolved supernatant was harvested, and total protein content was quantified using Pierce<sup>TM</sup> BCA Protein Assay Kit (Thermo Fisher Scientific, Rockford, IL, USA) following the manufacturer's instructions. Equal amounts of protein were mixed with 20  $\mu\text{L}$  of 10 mM L-DOPA and incubated at 37  $^{\circ}\text{C}$  for 1 h. Absorbance was measured at a wavelength of 490 nm using a microplate reader.

#### 4.6. PCR and Quantitative Real-Time PCR

B16F10 cells were cultured in 100 mm dishes. After incubation overnight, the cells were treated with different concentrations of LRE. Total RNA was extracted using the RiboEx reagent (Geneall Biotechnology, Seoul, Republic of Korea) as per the manufacturer's instructions. Synthesis of complementary DNA was performed using 1 µg of total RNA, oligo dT primers, 0.1 M DTT, 2.5 mM dNTPs, 5X First-Strand Buffer, and M-MLV reverse transcriptase (Thermo Fisher Scientific, Waltham, MA, USA). Glyceraldehyde-3-phosphate dehydrogenase (*Gapdh*) was used as a reference for the gene expression level normalization. The primer sequence for the specific gene analyzed is provided in Table 2.

**Table 2.** List of sequences used for PCR and qRT-PCR.

Target mRNA	Sequences of Primer	Amplicons (bp)	Annealing Temperature (°C)
<i>Gapdh</i>	F: 5'-CATCACTGCCACCCAGAAGACTG-3' R: 5'-ATGCCAGTGAGCTTCCCGTTCAG-3'	153	60
<i>Mitf</i>	F: 5'-AGAAGCTGGAGCATGCGAACC-3' R: 5'-GTTCTGGCTGCAGTTCTCAAG-3'	168	60
<i>Tyrosinase</i>	F: 5'-AGTCGTATCTGGCCATGGCTTCTTG-3' R: 5'-GCAAGCTGTGGTAGTCGTCTTTGTC-3'	169	60
<i>Tyrp1</i>	F: 5'-CTGCGATGCTGCACTGATGACTTG-3' R: 5'-TTTCTCCTGATTGGTCCACCCTCAG-3'	171	60
<i>Tyrp2</i>	F: 5'-GCTTGGATGACTACAACCGCCG-3' R: 5'-GGTGGGAAGAAGGGGACCATGT-3'	451	60

#### 4.7. Western Blot Analysis

B16F10 cells ( $0.5 \times 10^5$  cells/mL) were seeded in a 60 mm plate and cultured for 24 h. The cells treated with indicated concentrations of LRE and  $\alpha$ -MSH were lysed in Radioimmunoprecipitation (RIPA) assay buffer. The total protein content was measured by Pierce BCA Protein Assay Kit (Thermo Fisher Scientific). Proteins were loaded via 8% or 10% sodium dodecyl sulfate polyacrylamide gel electrophoresis (SDS-PAGE) and transferred to a nitrocellulose membrane. The membrane was blocked with 5% skim milk and incubated overnight at 4 °C with primary antibodies. The blots were incubated with horseradish peroxidase-conjugated anti-mouse IgG (#7076S; Cell Signaling Technology; CST; Danvers, MA, USA) or anti-rabbit IgG (#7074S; CST) secondary antibodies. Proteins were detected with ECL reagent (Bio-Rad) and visualized by the ChemiDoc Touch Imaging System (Bio-Rad, Hercules, CA, USA). The protein samples 20 µg protein samples were examined via Western blotting with the corresponding antibodies. All antibodies were purchased from Santa Cruz (Dallas, TX, USA) or CST. The following antibodies are listed in Table 3.

**Table 3.** List of primary antibodies for Western blot analyses.

Antigen	Host	Clonality (Species Reactivity)	Dilution	Manufacturer (Cat. Number)	References
Mitf	Mouse	Monoclonal (mouse, rat, human)	1:200	Santa Cruz (#sc-56725)	[102,103]
Tyrosinase	Mouse	Monoclonal (mouse, rat, human)	1:200	Santa Cruz (#sc-20035)	[102,104]
Tyrp1	Mouse	Monoclonal (mouse, rat, human)	1:200	Santa Cruz (#sc-166857)	[105,106]
Tyrp2	Mouse	Monoclonal (mouse, rat, human)	1:200	Santa Cruz (#sc-74439)	[107,108]

Table 3. Cont.

Antigen	Host	Clonality (Species Reactivity)	Dilution	Manufacturer (Cat. Number)	References
$\beta$ -actin	Mouse	Monoclonal (mouse, rat, human)	1:1000	Santa Cruz (#sc-47778)	[109,110]
PKA	Rabbit	Polyclonal (mouse, rat, human)	1:1000	CST (#4782S)	[111,112]
Phospho-PKA (Thr198)	Rabbit	Polyclonal (mouse, rat, human)	1:1000	CST (#4781S)	[112,113]
CREB	Rabbit	Monoclonal (mouse, rat, human...)	1:1000	CST(#9197S)	[31,114]
Phospho- CREB (Ser133)	Rabbit	Monoclonal (mouse, rat, human...)	1:1000	CST (#9198S)	[31,109]
ERK	Rabbit	Polyclonal (mouse, rat, human...)	1:1000	CST (#9102S)	[106,115]
Phospho-ERK (Thr202/Tyr204)	Rabbit	Polyclonal (mouse, rat, human...)	1:1000	CST (#9101S)	[106,115]
p38	Rabbit	Polyclonal (mouse, rat, human...)	1:1000	CST (#9212S)	[116,117]
Phospho-p38 (Thr180/Tyr182)	Rabbit	Polyclonal (mouse, rat, human...)	1:1000	CST (#9211S)	[111,116]

#### 4.8. Statistical Analysis

Data was analyzed by one-way analysis of variance (ANOVA) to determine the statistical significance of variations among the treatment groups. Subsequently, in instances where statistically significant treatment effects were detected, Tukey's test was used for comparisons between the means of multiple groups. The data are expressed as the mean  $\pm$  standard deviation (SD). Statistical significance was attributed to differences with  $p < 0.05$ .

**Supplementary Materials:** The following supporting information can be downloaded at <https://www.mdpi.com/article/10.3390/plants12213666/s1>. Figure S1: Effects of *Lilium lancifolium* (*L. lancifolium*) root extract on melanogenesis-related genes in B16F10 cells. (A) B16F10 cells were treated with the indicated concentrations of LRE and  $\alpha$ -MSH for 24 h. mRNA levels of tyrosinase-related genes (*tyrosinase*, *Tyrp1*, and *Tyrp2*) were detected via qRT-PCR, with *Gapdh* serving as a loading control. (B) B16F10 cells were seeded in 60-mm dishes ( $2 \times 10^5$  cells) and incubated for 24 h. The cells were treated with the indicated concentrations of LRE and  $\alpha$ -MSH for 24 h. The mRNA levels of *Mitf* were detected via qRT-PCR, with *Gapdh* serving as a loading control. The results are presented as the mean  $\pm$  SD of three independent experiments and were analyzed using a one-way analysis of variance followed by Tukey's test. qRT-PCR, quantitative real-time polymerase chain reaction; mRNA, messenger RNA, *Mitf*, microphthalmia-associated transcription factor. ###, \*\*\*  $p < 0.001$ , \*\*  $p < 0.01$ , \*  $p < 0.05$ .

**Author Contributions:** Conceptualization, S.P., J.L., S.A. and S.B.; methodology, S.P. and N.H.; software, S.P. and N.H.; validation, S.P., N.H., J.L., J.-N.L., S.A. and S.B.; formal analysis, S.P. and N.H.; investigation, S.P., N.H., J.L., J.-N.L., S.A. and S.B.; resources, S.A.; data curation, S.P. and N.H.; writing—original draft preparation, S.P. and S.B.; writing—review and editing, S.P., N.H., J.L., J.-N.L., S.A. and S.B.; visualization, S.P. and S.B.; supervision, S.B.; project administration, S.B.; funding acquisition, S.B. All authors have read and agreed to the published version of the manuscript.

**Funding:** This work was supported by the Commercializations Promotion Agency for R&D Outcomes (COMPA) grant funded by the Korean government (MSIT) (No. 2021B401).

**Data Availability Statement:** Not applicable.

**Acknowledgments:** The authors are grateful to the Department of Cosmetics Engineering, Konkuk University, for supporting the use of research facilities.

**Conflicts of Interest:** The authors declare no conflict of interest.

## References

1. Brenner, M.; Hearing, V.J. The protective role of melanin against UV damage in human skin. *Photochem. Photobiol.* **2008**, *84*, 539–549. [[CrossRef](#)] [[PubMed](#)]
2. Montagna, W.; Carlisle, K. The architecture of black and white facial skin. *J. Am. Acad. Dermatol.* **1991**, *24*, 929–937. [[CrossRef](#)] [[PubMed](#)]
3. Swalwell, H.; Latimer, J.; Haywood, R.M.; Birch-Machin, M.A. Investigating the role of melanin in UVA/UVB-and hydrogen peroxide-induced cellular and mitochondrial ROS production and mitochondrial DNA damage in human melanoma cells. *Free Radic. Biol. Med.* **2012**, *52*, 626–634. [[CrossRef](#)]
4. Bourhim, T.; Villareal, M.O.; Gadhi, C.; Hafidi, A.; Isoda, H. Depigmenting effect of argan press-cake extract through the down-regulation of Mitf and melanogenic enzymes expression in B16 murine melanoma cells. *Cytotechnology* **2018**, *70*, 1389–1397. [[CrossRef](#)] [[PubMed](#)]
5. Lerner, A.B.; Fitzpatrick, T.B. Biochemistry of melanin formation. *Physiol. Rev.* **1950**, *30*, 91–126. [[CrossRef](#)]
6. Ito, S.; Wakamatsu, K. Quantitative analysis of eumelanin and pheomelanin in humans, mice, and other animals: A comparative review. *Pigment Cell Res.* **2003**, *16*, 523–531. [[CrossRef](#)]
7. Thody, A.J.; Higgins, E.M.; Wakamatsu, K.; Ito, S.; Burchill, S.A.; Marks, J.M. Pheomelanin as well as eumelanin is present in human epidermis. *J. Invest. Dermatol.* **1991**, *97*, 340–344. [[CrossRef](#)]
8. Zanetti, R.; Prota, G.; Napolitano, A.; Martinez, C.; Sancho-Garnier, H.; Østerlind, A.; Sacerdote, C.; Rosso, S. Development of an integrated method of skin phenotype measurement using the melanins. *Melanoma Res.* **2001**, *11*, 551–557. [[CrossRef](#)]
9. Chung, K.W.; Park, Y.J.; Choi, Y.J.; Park, M.H.; Ha, Y.M.; Uehara, Y.; Yoon, J.H.; Chun, P.; Moon, H.R.; Chung, H.Y. Evaluation of in vitro and in vivo anti-melanogenic activity of a newly synthesized strong tyrosinase inhibitor (E)-3-(2, 4 dihydroxybenzylidene) pyrrolidine-2, 5-dione (3-DBP). *Biochim. Et. Biophys. Acta BBA-Gen. Subj.* **2012**, *1820*, 962–969. [[CrossRef](#)]
10. Riley, P.A. Melanogenesis and melanoma. *Pigment Cell Res.* **2003**, *16*, 548–552. [[CrossRef](#)]
11. Abdel-Daim, M.; Funasaka, Y.; Komoto, M.; Nakagawa, Y.; Yanagita, E.; Nishigori, C. Pharmacogenomics of metabotropic glutamate receptor subtype 1 and in vivo malignant melanoma formation. *J. Dermatol.* **2010**, *37*, 635–646. [[CrossRef](#)]
12. Miyamura, Y.; Coelho, S.G.; Wolber, R.; Miller, S.A.; Wakamatsu, K.; Zmudzka, B.Z.; Ito, S.; Smuda, C.; Passeron, T.; Choi, W. Regulation of human skin pigmentation and responses to ultraviolet radiation. *Pigment Cell Res.* **2007**, *20*, 2–13. [[CrossRef](#)] [[PubMed](#)]
13. Briganti, S.; Camera, E.; Picardo, M. Chemical and instrumental approaches to treat hyperpigmentation. *Pigment Cell Res.* **2003**, *16*, 101–110. [[CrossRef](#)]
14. Ruiz-Maldonado, R.; Orozco-Covarrubias, M.d.I.L. Postinflammatory hypopigmentation and hyperpigmentation. In Proceedings of the Seminars in Cutaneous Medicine and Surgery; WB Saunders Co.: Philadelphia, PA, USA, 1997; pp. 36–43.
15. Fistarol, S.K.; Itin, P.H. Disorders of pigmentation. *JDDG J. Der Dtsch. Dermatol. Ges.* **2010**, *8*, 187–202. [[CrossRef](#)] [[PubMed](#)]
16. Solano, F.; Briganti, S.; Picardo, M.; Ghanem, G. Hypopigmenting agents: An updated review on biological, chemical and clinical aspects. *Pigment Cell Res.* **2006**, *19*, 550–571. [[CrossRef](#)] [[PubMed](#)]
17. Rigopoulos, D.; Gregoriou, S.; Katsambas, A. Hyperpigmentation and melasma. *J. Cosmet. Dermatol.* **2007**, *6*, 195–202. [[CrossRef](#)] [[PubMed](#)]
18. Behrooz, K. Skin Depigmenting Agents: Where Do We Stand? In *Pigmentation Disorders*; Shahin, A., Ed.; IntechOpen: Rijeka, Croatia, 2022; p. Ch. 5.
19. Thody, A.J.; Graham, A. Does  $\alpha$ -MSH Have a Role in Regulating Skin Pigmentation in Humans? *Pigment Cell Res.* **1998**, *11*, 265–274. [[CrossRef](#)] [[PubMed](#)]
20. Nylander, K.; Bourdon, J.C.; Bray, S.E.; Gibbs, N.K.; Kay, R.; Hart, I.; Hall, P.A. Transcriptional activation of tyrosinase and TRP-1 by p53 links UV irradiation to the protective tanning response. *J. Pathol.* **2000**, *190*, 39–46. [[CrossRef](#)]
21. Cui, F.; She, X.D.; Li, X.F.; Shen, Y.N.; Lü, G.X.; Liu, W.D. Effects of Malassezia isolates on cytokines production associated with melanogenesis by keratinocytes. *Zhongguo Yi Xue Ke Xue Yuan Xue Bao Acta Acad. Med. Sin.* **2007**, *29*, 196–200.
22. Liyanage, A.; Liyanage, G.; Sirimanna, G.; Schürer, N. Comparative Study on Depigmenting Agents in Skin of Color. *J. Clin. Aesthetic Dermatol.* **2022**, *15*, 12–17.
23. Sarkar, R.; Arora, P.; Garg, K.V. Cosmeceuticals for Hyperpigmentation: What is Available? *J. Cutan. Aesthetic Surg.* **2013**, *6*, 4–11. [[CrossRef](#)] [[PubMed](#)]
24. Pillaiyar, T.; Manickam, M.; Jung, S.-H. Recent development of signaling pathways inhibitors of melanogenesis. *Cell. Signal.* **2017**, *40*, 99–115. [[CrossRef](#)]
25. Zheng, Y.; Du, X.; Zhang, L.; Jia, T.; Zhang, H.; Peng, B.; Hao, Y.; Tong, Z.; Che, D.; Geng, S. Hydroquinone-induced skin irritant reaction could be achieved by activating mast cells via mas-related G protein-coupled receptor X2. *Exp. Dermatol.* **2023**, *32*, 436–446. [[CrossRef](#)]

26. Nordlund, J.J.; Grimes, P.E.; Ortonne, J.P. The safety of hydroquinone. *J. Eur. Acad. Dermatol. Venereol.* **2006**, *20*, 781–787. [[CrossRef](#)] [[PubMed](#)]
27. Nakagawa, M.; Kawai, K.; Kawai, K. Contact allergy to kojic acid in skin care products. *Contact Dermat.* **1995**, *32*, 9–13. [[CrossRef](#)] [[PubMed](#)]
28. Ebanks, J.P.; Wickett, R.R.; Boissy, R.E. Mechanisms regulating skin pigmentation: The rise and fall of complexion coloration. *Int. J. Mol. Sci.* **2009**, *10*, 4066–4087. [[CrossRef](#)] [[PubMed](#)]
29. Ishack, S.; Lipner, S.R. Exogenous ochronosis associated with hydroquinone: A systematic review. *Int. J. Dermatol.* **2022**, *61*, 675–684. [[CrossRef](#)]
30. Jow, T.; Hantash, B.M. Hydroquinone-Induced Depigmentation: Case Report and Review of the Literature. *Dermatitis* **2014**, *25*, e1–e5. [[CrossRef](#)]
31. Ahn, M.J.; Hur, S.J.; Kim, E.H.; Lee, S.H.; Shin, J.S.; Kim, M.K.; Uchizono, J.A.; Whang, W.K.; Kim, D.S. Scopoletin from *Cirsium setidens* Increases Melanin Synthesis via CREB Phosphorylation in B16F10 Cells. *Korean J. Physiol. Pharmacol. Off. J. Korean Physiol. Soc. Korean Soc. Pharmacol.* **2014**, *18*, 307–311. [[CrossRef](#)]
32. Schwartz, C.; Jan, A.; Zito, P.M. Hydroquinone. In *StatPearls*; StatPearls Publishing: St. Petersburg, FL, USA, 2023.
33. Nautiyal, A.; Wairkar, S. Management of hyperpigmentation: Current treatments and emerging therapies. *Pigment Cell Melanoma Res.* **2021**, *34*, 1000–1014. [[CrossRef](#)]
34. Draelos, Z.D. Skin lightening preparations and the hydroquinone controversy. *Dermatol. Ther.* **2007**, *20*, 308–313. [[CrossRef](#)] [[PubMed](#)]
35. Mishima, Y.; Hatta, S.; Ohyama, Y.; Inazu, M. Induction of melanogenesis suppression: Cellular pharmacology and mode of differential action. *Pigment Cell Res.* **1988**, *1*, 367–374. [[CrossRef](#)] [[PubMed](#)]
36. Parvez, S.; Kang, M.; Chung, H.S.; Cho, C.; Hong, M.C.; Shin, M.K.; Bae, H. Survey and mechanism of skin depigmenting and lightening agents. *Phytother. Res. Int. J. Devoted Pharmacol. Toxicol. Eval. Nat. Prod. Deriv.* **2006**, *20*, 921–934. [[CrossRef](#)]
37. Maeda, K.; Fukuda, M. Arbutin: Mechanism of its depigmenting action in human melanocyte culture. *J. Pharmacol. Exp. Ther.* **1996**, *276*, 765–769.
38. Halder, R.M.; Nordlund, J.J. Topical treatment of pigmentary disorders. In *The Pigmentary System: Physiology and Pathophysiology*; Blackwell Publishing Ltd.: Hoboken, NJ, USA, 2006; pp. 1163–1174.
39. Garcia, A.; Fulton, J.E., Jr. The combination of glycolic acid and hydroquinone or kojic acid for the treatment of melasma and related conditions. *Dermatol. Surg.* **1996**, *22*, 443–447. [[CrossRef](#)]
40. Cardoso, R.; Valente, R.; Souza da Costa, C.H.; da S. Gonçalves Vianez, J.L., Jr.; Santana da Costa, K.; de Molfetta, F.A.; Nahum Alves, C. Analysis of Kojic Acid Derivatives as Competitive Inhibitors of Tyrosinase: A Molecular Modeling Approach. *Molecules* **2021**, *26*, 2875. [[CrossRef](#)] [[PubMed](#)]
41. Chung, Y.C.; Hyun, C.-G. Inhibitory Effects of Pinostilbene Hydrate on Melanogenesis in B16F10 Melanoma Cells via ERK and p38 Signaling Pathways. *Int. J. Mol. Sci.* **2020**, *21*, 4732. [[CrossRef](#)] [[PubMed](#)]
42. Lim, J.T.E.; Frcpi. Treatment of melasma using kojic acid in a gel containing hydroquinone and glycolic acid. *Dermatol. Surg.* **1999**, *25*, 282–284. [[CrossRef](#)] [[PubMed](#)]
43. Wei, C.; Huang, T.; Fernando, S.; Chung, K. Mutagenicity studies of kojic acid. *Toxicol. Lett.* **1991**, *59*, 213–220. [[CrossRef](#)]
44. Qian, W.; Liu, W.; Zhu, D.; Cao, Y.; Tang, A.; Gong, G.; Su, H. Natural skin-whitening compounds for the treatment of melanogenesis. *Exp. Ther. Med.* **2020**, *20*, 173–185. [[CrossRef](#)]
45. Chiang, H.-M.; Chien, Y.-C.; Wu, C.-H.; Kuo, Y.-H.; Wu, W.-C.; Pan, Y.-Y.; Su, Y.-H.; Wen, K.-C. Hydroalcoholic extract of *Rhodiola rosea* L. (Crassulaceae) and its hydrolysate inhibit melanogenesis in B16F0 cells by regulating the CREB/MITF/tyrosinase pathway. *Food Chem. Toxicol.* **2014**, *65*, 129–139. [[CrossRef](#)] [[PubMed](#)]
46. Zheng, Z.-P.; Cheng, K.-W.; Zhu, Q.; Wang, X.-C.; Lin, Z.-X.; Wang, M. Tyrosinase inhibitory constituents from the roots of *Morus nigra*: A structure—Activity relationship study. *J. Agric. Food Chem.* **2010**, *58*, 5368–5373. [[CrossRef](#)] [[PubMed](#)]
47. Sirat, H.M.; Rezali, M.F.; Ujang, Z. Isolation and identification of radical scavenging and tyrosinase inhibition of polyphenols from *Tibouchina semidecandra* L. *J. Agric. Food Chem.* **2010**, *58*, 10404–10409. [[CrossRef](#)]
48. Gao, J.; Zhang, T.; Jin, Z.-Y.; Xu, X.-M.; Wang, J.-H.; Zha, X.-Q.; Chen, H.-Q. Structural characterisation, physicochemical properties and antioxidant activity of polysaccharide from *Lilium lancifolium* Thunb. *Food Chem.* **2015**, *169*, 430–438. [[CrossRef](#)]
49. Zhang, T.; Gao, J.; Jin, Z.-Y.; Xu, X.-M.; Chen, H.-Q. Protective effects of polysaccharides from *Lilium lancifolium* on streptozotocin-induced diabetic mice. *Int. J. Biol. Macromol.* **2014**, *65*, 436–440. [[CrossRef](#)]
50. Wang, P.; Li, J.; Attia, F.A.K.; Kang, W.; Wei, J.; Liu, Z.; Li, C. A critical review on chemical constituents and pharmacological effects of *Lilium*. *Food Sci. Hum. Wellness* **2019**, *8*, 330–336. [[CrossRef](#)]
51. Kwon, O.-K.; Lee, M.-Y.; Yuk, J.-E.; Oh, S.-R.; Chin, Y.-W.; Lee, H.-K.; Ahn, K.-S. Anti-inflammatory effects of methanol extracts of the root of *Lilium lancifolium* on LPS-stimulated Raw264. 7 cells. *J. Ethnopharmacol.* **2010**, *130*, 28–34. [[CrossRef](#)] [[PubMed](#)]
52. You, X.; Xie, C.; Liu, K.; Gu, Z. Isolation of non-starch polysaccharides from bulb of tiger lily (*Lilium lancifolium* Thunb.) with fermentation of *Saccharomyces cerevisiae*. *Carbohydr. Polym.* **2010**, *81*, 35–40. [[CrossRef](#)]
53. Xue, C.C.; Shergis, J.L.; Zhang, A.L.; Worsnop, C.; Fong, H.; Story, D.; Da Costa, C.; Thien, F.C. Panax ginseng CA Meyer root extract for moderate chronic obstructive pulmonary disease (COPD): Study protocol for a randomised controlled trial. *Trials* **2011**, *12*, 164. [[CrossRef](#)]

54. Sun, X.; Gao, R.-L.; Xiong, Y.-K.; Huang, Q.-C.; Xu, M. Antitumor and immunomodulatory effects of a water-soluble polysaccharide from *Lilium Bulbus* in mice. *Carbohydr. Polym.* **2014**, *102*, 543–549. [[CrossRef](#)]
55. Cheng, A.; Wan, F.; Wang, J.; Jin, Z.; Xu, X. Macrophage immunomodulatory activity of polysaccharides isolated from *Glycyrrhiza uralensis* fish. *Int. Immunopharmacol.* **2008**, *8*, 43–50. [[CrossRef](#)] [[PubMed](#)]
56. Pan, G.; Xie, Z.; Huang, S.; Tai, Y.; Cai, Q.; Jiang, W.; Sun, J.; Yuan, Y. Immune-enhancing effects of polysaccharides extracted from *Lilium lancifolium* Thunb. *Int. Immunopharmacol.* **2017**, *52*, 119–126. [[CrossRef](#)] [[PubMed](#)]
57. Xu, Z.; Wang, H.; Wang, B.; Fu, L.; Yuan, M.; Liu, J.; Zhou, L.; Ding, C. Characterization and antioxidant activities of polysaccharides from the leaves of *Lilium lancifolium* Thunb. *Int. J. Biol. Macromol.* **2016**, *92*, 148–155. [[CrossRef](#)] [[PubMed](#)]
58. Sim, W.S.; Choi, S.I.; Jung, T.D.; Cho, B.Y.; Choi, S.H.; Park, S.M.; Lee, O.H. Antioxidant and anti-inflammatory effects of *Lilium lancifolium* bulbs extract. *J. Food Biochem.* **2020**, *44*, e13176. [[CrossRef](#)] [[PubMed](#)]
59. Lee, E.; Yun, N.; Jang, Y.P.; Kim, J. *Lilium lancifolium* Thunb. extract attenuates pulmonary inflammation and air space enlargement in a cigarette smoke-exposed mouse model. *J. Ethnopharmacol.* **2013**, *149*, 148–156. [[CrossRef](#)]
60. Park, T.; Seo, K.-S.; Choi, S.; Yun, K.W. Chemical Constituents of Bulb of *Lilium lancifolium* Thunberg and *Lilium tsingtauense* Gilg. *Korean J. Plant Resour.* **2014**, *27*, 125–132. [[CrossRef](#)]
61. Zhou, J.; An, R.; Huang, X. Genus *Lilium*: A review on traditional uses, phytochemistry and pharmacology. *J. Ethnopharmacol.* **2021**, *270*, 113852. [[CrossRef](#)]
62. Tang, Y.; Liu, Y.; Luo, K.; Xu, L.; Yang, P.; Ming, J. Potential Applications of *Lilium* Plants in Cosmetics: A Comprehensive Review Based on Research Papers and Patents. *Antioxidants* **2022**, *11*, 1458. [[CrossRef](#)]
63. Ferreira, A.M.; de Souza, A.A.; Koga, R.C.R.; Sena, I.D.S.; Matos, M.J.S.; Tomazi, R.; Ferreira, I.M.; Carvalho, J.C.T. Anti-Melanogenic Potential of Natural and Synthetic Substances: Application in Zebrafish Model. *Molecules* **2023**, *28*, 1053. [[CrossRef](#)]
64. Wang, R.; Tang, P.; Wang, P.; Boissy, R.E.; Zheng, H. Regulation of tyrosinase trafficking and processing by presenilins: Partial loss of function by familial Alzheimer's disease mutation. *Proc. Natl. Acad. Sci. USA* **2006**, *103*, 353–358. [[CrossRef](#)]
65. del Marmol, V.; Beermann, F. Tyrosinase and related proteins in mammalian pigmentation. *FEBS Lett.* **1996**, *381*, 165–168. [[CrossRef](#)]
66. Sun, M.; Xie, H.-F.; Tang, Y.; Lin, S.-Q.; Li, J.-M.; Sun, S.-N.; Hu, X.-L.; Huang, Y.-X.; Shi, W.; Jian, D. G protein-coupled estrogen receptor enhances melanogenesis via cAMP-protein kinase (PKA) by upregulating microphthalmia-related transcription factor-tyrosinase in melanoma. *J. Steroid Biochem. Mol. Biol.* **2017**, *165*, 236–246. [[CrossRef](#)]
67. Bentley, N.; Eisen, T.; Goding, C. Melanocyte-specific expression of the human tyrosinase promoter: Activation by the microphthalmia gene product and role of the initiator. *Mol. Cell. Biol.* **1994**, *14*, 7996–8006. [[PubMed](#)]
68. Vachtenheim, J.; Borovanský, J. "Transcription physiology" of pigment formation in melanocytes: Central role of MITF. *Exp. Dermatol.* **2010**, *19*, 617–627. [[CrossRef](#)] [[PubMed](#)]
69. Kim, S.S.; Kim, M.J.; Choi, Y.H.; Kim, B.K.; Kim, K.S.; Park, K.J.; Park, S.M.; Lee, N.H.; Hyun, C.G. Down-regulation of tyrosinase, TRP-1, TRP-2 and MITF expressions by citrus press-cakes in murine B16 F10 melanoma. *Asian Pac. J. Trop. Biomed.* **2013**, *3*, 617–622, discussion 621–612. [[CrossRef](#)] [[PubMed](#)]
70. Chan, C.-F.; Huang, C.-C.; Lee, M.-Y.; Lin, Y.-S. Fermented broth in tyrosinase-and melanogenesis inhibition. *Molecules* **2014**, *19*, 13122–13135. [[CrossRef](#)]
71. Kim, A.; Yim, N.-H.; Im, M.; Jung, Y.P.; Liang, C.; Cho, W.-K.; Ma, J.Y. Ssanhwa-tang, an oriental herbal cocktail, exerts anti-melanogenic activity by suppression of the p38 MAPK and PKA signaling pathways in B16F10 cells. *BMC Complement. Altern. Med.* **2013**, *13*, 214. [[CrossRef](#)]
72. Kim, Y.M.; Cho, S.E.; Seo, Y.K. The activation of melanogenesis by p-CREB and MITF signaling with extremely low-frequency electromagnetic fields on B16F10 melanoma. *Life Sci.* **2016**, *162*, 25–32. [[CrossRef](#)] [[PubMed](#)]
73. Hartman, M.L.; Czyz, M. MITF in melanoma: Mechanisms behind its expression and activity. *Cell. Mol. Life Sci.* **2015**, *72*, 1249–1260. [[CrossRef](#)]
74. Saha, B.; Singh, S.K.; Sarkar, C.; Bera, R.; Ratha, J.; Tobin, D.J.; Bhadra, R. Activation of the Mitf promoter by lipid-stimulated activation of p38-stress signalling to CREB. *Pigment Cell Res.* **2006**, *19*, 595–605. [[CrossRef](#)]
75. Zhang, H.; Kong, Q.; Wang, J.; Jiang, Y.; Hua, H. Complex roles of cAMP–PKA–CREB signaling in cancer. *Exp. Hematol. Oncol.* **2020**, *9*, 32. [[CrossRef](#)]
76. Wang, H.; Xu, J.; Lazarovici, P.; Quirion, R.; Zheng, W. cAMP Response Element-Binding Protein (CREB): A Possible Signaling Molecule Link in the Pathophysiology of Schizophrenia. *Front. Mol. Neurosci.* **2018**, *11*, 255. [[CrossRef](#)] [[PubMed](#)]
77. Ao, Y.; Park, H.Y.; Olaizola-Horn, S.; Gilcrest, B.A. Activation of cAMP-dependent protein kinase is required for optimal alpha-melanocyte-stimulating hormone-induced pigmentation. *Exp. Cell Res.* **1998**, *244*, 117–124. [[CrossRef](#)]
78. Roh, E.; Yun, C.-Y.; Young Yun, J.; Park, D.; Doo Kim, N.; Yeon Hwang, B.; Jung, S.-H.; Park, S.K.; Kim, Y.-B.; Han, S.-B.; et al. cAMP-Binding Site of PKA as a Molecular Target of Bisabolangelone against Melanocyte-Specific Hyperpigmented Disorder. *J. Investig. Dermatol.* **2013**, *133*, 1072–1079. [[CrossRef](#)]
79. Herraiz, C.; Journé, F.; Abdel-Malek, Z.; Ghanem, G.; Jiménez-Cervantes, C.; García-Borrón, J.C. Signaling from the Human Melanocortin 1 Receptor to ERK1 and ERK2 Mitogen-Activated Protein Kinases Involves Transactivation of cKIT. *Mol. Endocrinol.* **2011**, *25*, 138–156. [[CrossRef](#)]
80. Ge, Y.C.; Li, J.N.; Ni, X.T.; Guo, C.M.; Wang, W.S.; Duan, T.; Sun, K. Cross talk between cAMP and p38 MAPK pathways in the induction of leptin by hCG in human placental syncytiotrophoblasts. *Reproduction* **2011**, *142*, 369–375. [[CrossRef](#)]

81. Delghandi, M.P.; Johannessen, M.; Moens, U. The cAMP signalling pathway activates CREB through PKA, p38 and MSK1 in NIH 3T3 cells. *Cell. Signal.* **2005**, *17*, 1343–1351. [[CrossRef](#)] [[PubMed](#)]
82. Bang, J.; Zippin, J.H. Cyclic adenosine monophosphate (cAMP) signaling in melanocyte pigmentation and melanomagenesis. *Pigment Cell Melanoma Res.* **2021**, *34*, 28–43. [[CrossRef](#)]
83. Raker, V.K.; Becker, C.; Steinbrink, K. The cAMP Pathway as Therapeutic Target in Autoimmune and Inflammatory Diseases. *Front. Immunol.* **2016**, *7*, 123. [[CrossRef](#)] [[PubMed](#)]
84. Englaro, W.; Rezzonico, R.; Durand-Clément, M.; Lallemand, D.; Ortonne, J.-P.; Ballotti, R. Mitogen-activated Protein Kinase Pathway and AP-1 Are Activated during cAMP-induced Melanogenesis in B-16 Melanoma Cells (\*). *J. Biol. Chem.* **1995**, *270*, 24315–24320. [[CrossRef](#)]
85. Sassone-Corsi, P. The cyclic AMP pathway. *Cold Spring Harb. Perspect. Biol.* **2012**, *4*, a011148. [[CrossRef](#)]
86. Buscà, R.; Ballotti, R. Cyclic AMP a Key Messenger in the Regulation of Skin Pigmentation. *Pigment Cell Res.* **2000**, *13*, 60–69. [[CrossRef](#)]
87. Slominski, A.; Zmijewski, M.A.; Pawelek, J. L-tyrosine and L-dihydroxyphenylalanine as hormone-like regulators of melanocyte functions. *Pigment Cell Melanoma Res.* **2012**, *25*, 14–27. [[CrossRef](#)]
88. Yuan, Z.Y.; Li, Z.Y.; Zhao, H.Q.; Gao, C.; Xiao, M.W.; Jiang, X.M.; Zhu, J.P.; Huang, H.Y.; Xu, G.M.; Xie, M.Z. Effects of different drying methods on the chemical constituents of *Lilium lancifolium* Thunb. based on UHPLC-MS analysis and antidepressant activity of the main chemical component regaloside A. *J. Sep. Sci.* **2021**, *44*, 992–1004. [[CrossRef](#)]
89. Farishian, R.A.; Wittaker, J.H. Phenylalanine Lowers Melanin Synthesis in Mammalian Melanocytes by Reducing Tyrosinase Uptake: Implications for Pigment Reduction in Phenylketonuria. *J. Investig. Dermatol.* **1980**, *74*, 85–89. [[CrossRef](#)]
90. Kaushik, N.; Kim, J.H.; Nguyen, L.N.; Kaushik, N.K.; Choi, K.A. Characterization of Bioactive Compounds Having Antioxidant and Anti-Inflammatory Effects of Liliaceae Family Flower Petal Extracts. *J. Funct. Biomater.* **2022**, *13*, 284. [[CrossRef](#)]
91. Costin, G.E.; Hearing, V.J. Human skin pigmentation: Melanocytes modulate skin color in response to stress. *FASEB J. Off. Publ. Fed. Am. Soc. Exp. Biol.* **2007**, *21*, 976–994. [[CrossRef](#)]
92. Yardman-Frank, J.M.; Fisher, D.E. Skin pigmentation and its control: From ultraviolet radiation to stem cells. *Exp. Dermatol.* **2021**, *30*, 560–571. [[CrossRef](#)]
93. Thawabteh, A.M.; Jibreen, A.; Karaman, D.; Thawabteh, A.; Karaman, R. Skin Pigmentation Types, Causes and Treatment-A Review. *Molecules* **2023**, *28*, 4839. [[CrossRef](#)]
94. Searle, T.; Al-Niaimi, F.; Ali, F.R. The top 10 cosmeceuticals for facial hyperpigmentation. *Dermatol. Ther.* **2020**, *33*, e14095. [[CrossRef](#)]
95. Bertolotto, C.; Buscà, R.; Abbe, P.; Bille, K.; Aberdam, E.; Ortonne, J.P.; Ballotti, R. Different cis-acting elements are involved in the regulation of TRP1 and TRP2 promoter activities by cyclic AMP: Pivotal role of M boxes (GTCATGTGCT) and of microphthalmia. *Mol. Cell. Biol.* **1998**, *18*, 694–702. [[CrossRef](#)]
96. Huang, H.C.; Chang, S.J.; Wu, C.Y.; Ke, H.J.; Chang, T.M. [6]-Shogaol inhibits  $\alpha$ -MSH-induced melanogenesis through the acceleration of ERK and PI3K/Akt-mediated MITF degradation. *BioMed Res. Int.* **2014**, *2014*, 842569. [[CrossRef](#)] [[PubMed](#)]
97. Lee, H.J.; An, S.; Bae, S.; Lee, J.H. Diarylpropionitrile inhibits melanogenesis via protein kinase A/cAMP-response element-binding protein/microphthalmia-associated transcription factor signaling pathway in  $\alpha$ -MSH-stimulated B16F10 melanoma cells. *Korean J. Physiol. Pharmacol. Off. J. Korean Physiol. Soc. Korean Soc. Pharmacol.* **2022**, *26*, 113–123. [[CrossRef](#)] [[PubMed](#)]
98. Nam, G.; An, S.K.; Park, I.C.; Bae, S.; Lee, J.H. Daphnetin inhibits  $\alpha$ -MSH-induced melanogenesis via PKA and ERK signaling pathways in B16F10 melanoma cells. *Biosci. Biotechnol. Biochem.* **2022**, *86*, 596–609. [[CrossRef](#)] [[PubMed](#)]
99. Zhang, A.; Zhao, R.; Wang, Y.; Liu, T.; Tian, H.; Yin, X.; Yang, L.; Sui, X. Natural surfactant used as an additive in the homogenate-ultrasound-synergistic extraction of regaloside A and polysaccharides from *Lilium lancifolium* bulbs using Doehlert matrix design. *Ind. Crops Prod.* **2022**, *188*, 115689. [[CrossRef](#)]
100. Park, S.; Han, N.; Lee, J.-M.; Lee, J.-H.; Bae, S. Effects of *Allium hookeri* Extracts on Hair-Inductive and Anti-Oxidative Properties in Human Dermal Papilla Cells. *Plants* **2023**, *12*, 1919. [[CrossRef](#)]
101. Ullah, S.; Chung, Y.C.; Hyun, C.G. Induction of Melanogenesis by Fosfomycin in B16F10 Cells Through the Upregulation of P-JNK and P-p38 Signaling Pathways. *Antibiotics* **2020**, *9*, 172. [[CrossRef](#)]
102. Kim, M.J.; Mohamed, E.A.; Kim, D.S.; Park, M.J.; Ahn, B.J.; Jeung, E.B.; An, B.S. Inhibitory effects and underlying mechanisms of *Artemisia capillaris* essential oil on melanogenesis in the B16F10 cell line. *Mol. Med. Rep.* **2022**, *25*, 113. [[CrossRef](#)]
103. Waku, T.; Nakada, S.; Masuda, H.; Sumi, H.; Wada, A.; Hirose, S.; Aketa, I.; Kobayashi, A. The CNC-family transcription factor Nrf3 coordinates the melanogenesis cascade through macropinocytosis and autophagy regulation. *Cell Rep.* **2023**, *42*, 111906. [[CrossRef](#)]
104. Yu, B.Y.; Ngo, H.H.; Choi, W.J.; Keum, Y.S. Dimethyl Itaconate Inhibits Melanogenesis in B16F10 Cells. *Antioxidants* **2023**, *12*, 692. [[CrossRef](#)]
105. Joo, I.H.; Choi, J.H.; Kim, D.H.; Chung, M.J.; Lim, M.H. *Ligularia fischeri* ethanol extract: An inhibitor of alpha-melanocyte-stimulating hormone-stimulated melanogenesis in B16F10 melanoma cells. *J. Cosmet. Dermatol.* **2023**, *22*, 637–644. [[CrossRef](#)]
106. Shin, S.; Ko, J.; Kim, M.; Song, N.; Park, K. Morin Induces Melanogenesis via Activation of MAPK Signaling Pathways in B16F10 Mouse Melanoma Cells. *Molecules* **2021**, *26*, 2150. [[CrossRef](#)] [[PubMed](#)]
107. Lee, J.H.; Lee, B.; Jeon, Y.D.; Song, H.W.; Lee, Y.M.; Song, B.J.; Kim, D.K. Inhibitory Effect of *Elaeagnus umbellata* Fractions on Melanogenesis in  $\alpha$ -MSH-Stimulated B16-F10 Melanoma Cells. *Molecules* **2021**, *26*, 1308. [[CrossRef](#)] [[PubMed](#)]

108. Yang, S.H.; Tsatsakis, A.M.; Tzanakakis, G.; Kim, H.S.; Le, B.; Sifaki, M.; Spandidos, D.A.; Tsukamoto, C.; Golokhvast, K.S.; Izotov, B.N.; et al. Soyasaponin Ag inhibits  $\alpha$ -MSH-induced melanogenesis in B16F10 melanoma cells via the downregulation of TRP-2. *Int. J. Mol. Med.* **2017**, *40*, 631–636. [[CrossRef](#)]
109. Zhou, X.; Oh, J.H.; Karadeniz, F.; Yang, J.; Lee, H.; Seo, Y.; Kong, C.-S. Anti-Melanogenesis Effect of Rosa rugosa on  $\alpha$ -MSH-Induced B16F10 Cells via PKA/CREB Pathway Activation. *Appl. Sci.* **2023**, *13*, 184.
110. Lee, K.R.; Lee, J.S.; Lee, S.; Son, Y.K.; Kim, G.R.; Sim, Y.C.; Song, J.E.; Ha, S.J.; Hong, E.K. Polysaccharide isolated from the liquid culture broth of Inonotus obliquus suppresses invasion of B16-F10 melanoma cells via AKT/NF- $\kappa$ B signaling pathway. *Mol. Med. Rep.* **2016**, *14*, 4429–4435. [[CrossRef](#)]
111. Han, H.; Hyun, C. Acenocoumarol, an Anticoagulant Drug, Prevents Melanogenesis in B16F10 Melanoma Cells. *Pharmaceuticals* **2023**, *16*, 604. [[CrossRef](#)]
112. Kim, H.M.; Hyun, C.G. Miglitol, an Oral Antidiabetic Drug, Downregulates Melanogenesis in B16F10 Melanoma Cells through the PKA, MAPK, and GSK3 $\beta$ / $\beta$ -Catenin Signaling Pathways. *Molecules* **2022**, *28*, 115. [[CrossRef](#)]
113. Lee, H.J.; Kim, S.H.; Kim, Y.H.; Kim, S.H.; Oh, G.S.; Bae, J.E.; Kim, J.B.; Park, N.Y.; Park, K.; Yeom, E.; et al. Nalfurafine Hydrochloride, a  $\kappa$ -Opioid Receptor Agonist, Induces Melanophagy via PKA Inhibition in B16F1 Cells. *Cells* **2022**, *12*, 146. [[CrossRef](#)]
114. Choi, M.R.; Lee, H.; Kim, H.K.; Han, J.; Seol, J.E.; Vasileva, E.A.; Mishchenko, N.P.; Fedoreyev, S.A.; Stonik, V.A.; Ju, W.S.; et al. Echinochrome A Inhibits Melanogenesis in B16F10 Cells by Downregulating CREB Signaling. *Mar. Drugs* **2022**, *20*, 555. [[CrossRef](#)]
115. Yao, C.; Jin, C.L.; Oh, J.H.; Oh, I.G.; Park, C.H.; Chung, J.H. Ardisia crenata extract stimulates melanogenesis in B16F10 melanoma cells through inhibiting ERK1/2 and Akt activation. *Mol. Med. Rep.* **2015**, *11*, 653–657. [[CrossRef](#)] [[PubMed](#)]
116. Song, M.; Lee, J.; Kim, Y.J.; Hoang, D.H.; Choe, W.; Kang, I.; Kim, S.S.; Ha, J. Jeju Magma-Seawater Inhibits  $\alpha$ -MSH-Induced Melanogenesis via CaMKK $\beta$ -AMPK Signaling Pathways in B16F10 Melanoma Cells. *Mar. Drugs* **2020**, *18*, 473. [[CrossRef](#)] [[PubMed](#)]
117. Huang, H.C.; Lin, H.; Huang, M.C. The lactoferrin B-derived peptide, LfB17-34, induces melanogenesis in B16F10 cells. *Int. J. Mol. Med.* **2017**, *39*, 595–602. [[CrossRef](#)] [[PubMed](#)]

**Disclaimer/Publisher's Note:** The statements, opinions and data contained in all publications are solely those of the individual author(s) and contributor(s) and not of MDPI and/or the editor(s). MDPI and/or the editor(s) disclaim responsibility for any injury to people or property resulting from any ideas, methods, instructions or products referred to in the content.